Sparse Variational Computing at the Quantum Edge of Chaos

D. Jaksch, University of Hamburg

QCFD (qcfd-h2020.eu)

EU HORIZON-CL4-2021-DIGITAL-EMERGING-02-10
grant agreement No. 101080085 QCFD

Universität Hamburg
DER FORSCHUNG | DER LEHRE | DER BILDUNG

Grenoble, 8th October 2025

Hybrid Classical-Quantum Optimization – Architecture

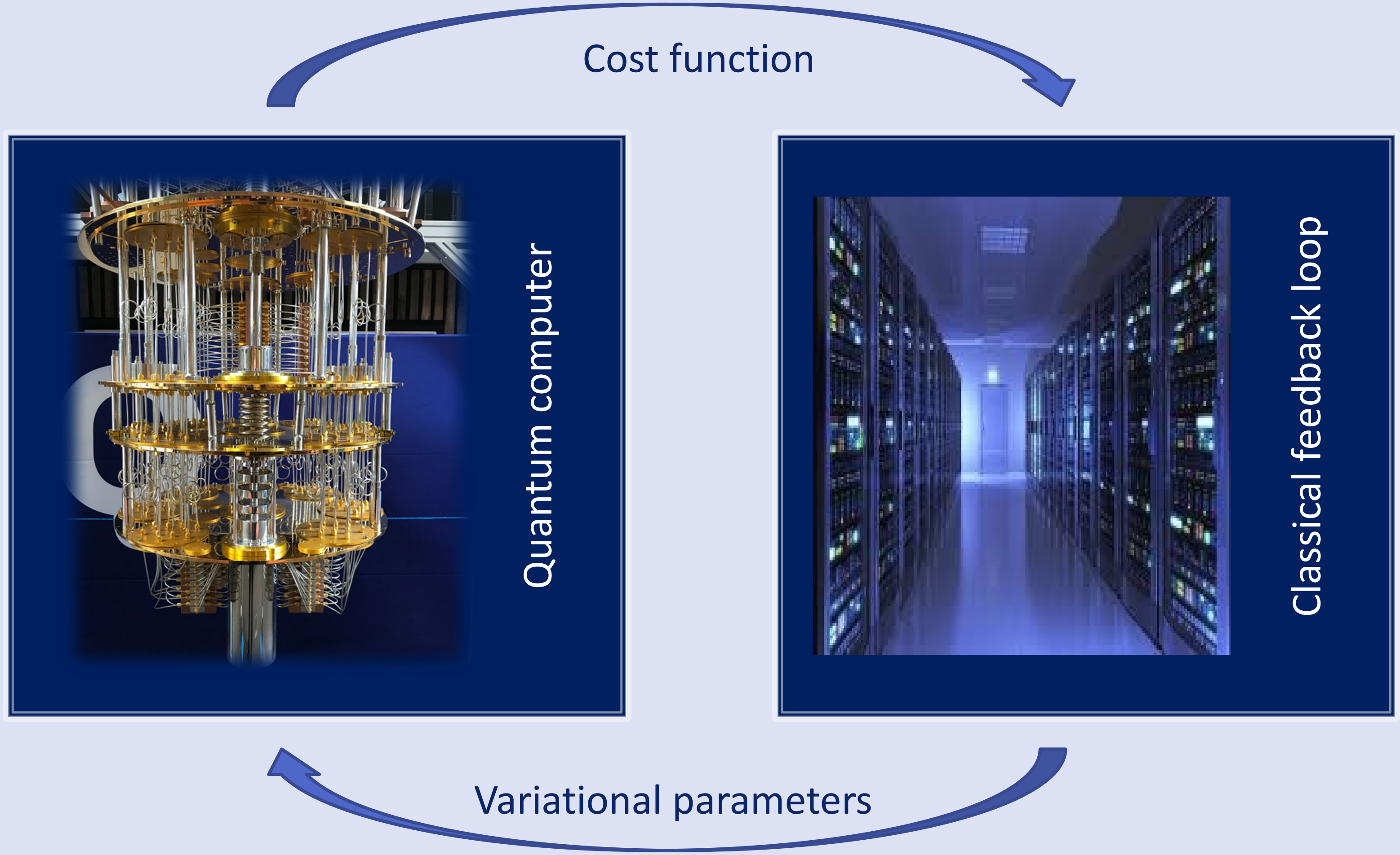

A. Peruzzo, et al., Nat. Commun. **5**, 4213 (2014).

Hybrid Classical-Quantum Optimization – Architecture

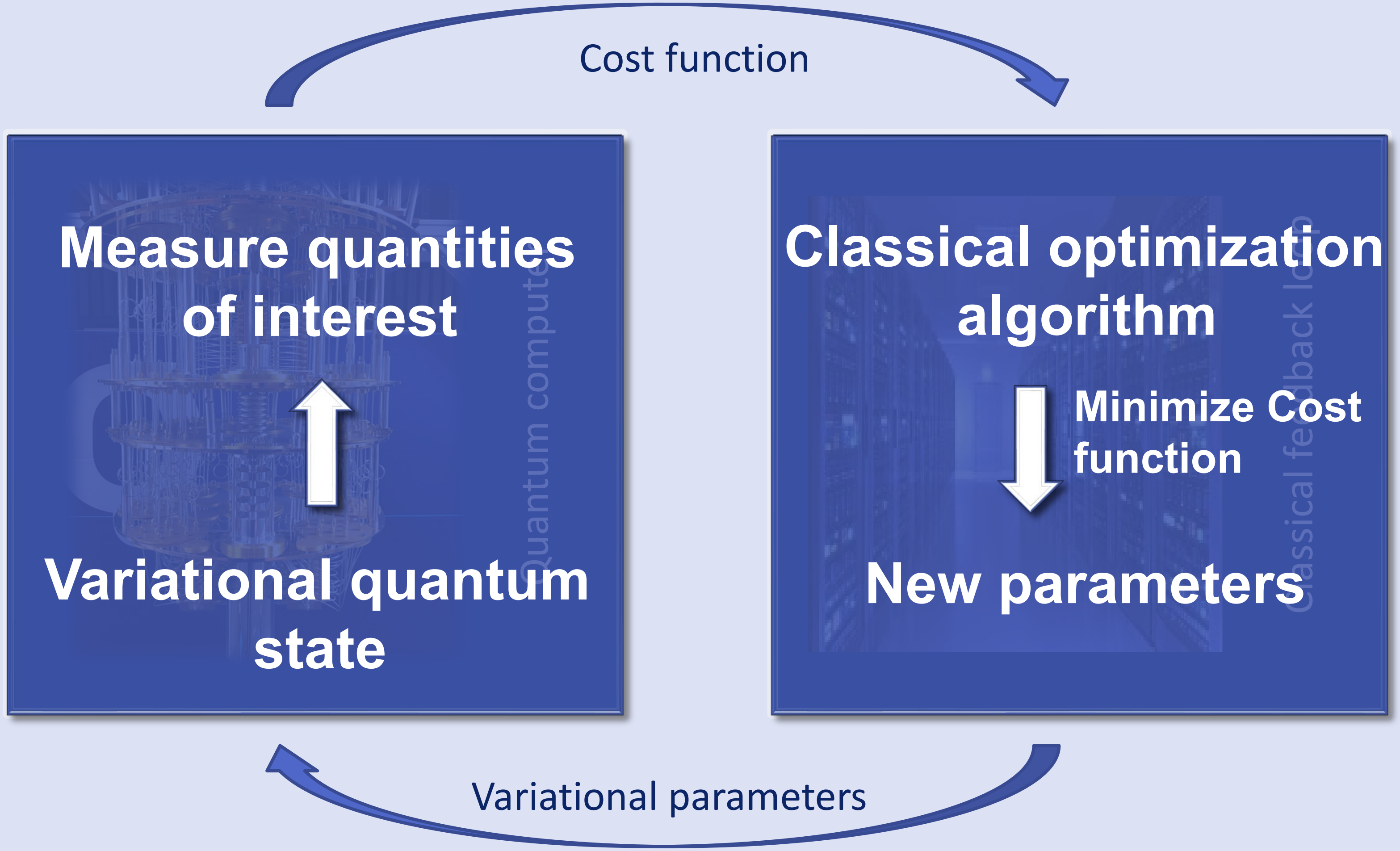

A. Peruzzo, et al., Nat. Commun. **5**, 4213 (2014).

Hybrid Classical-Quantum Optimization – Architecture

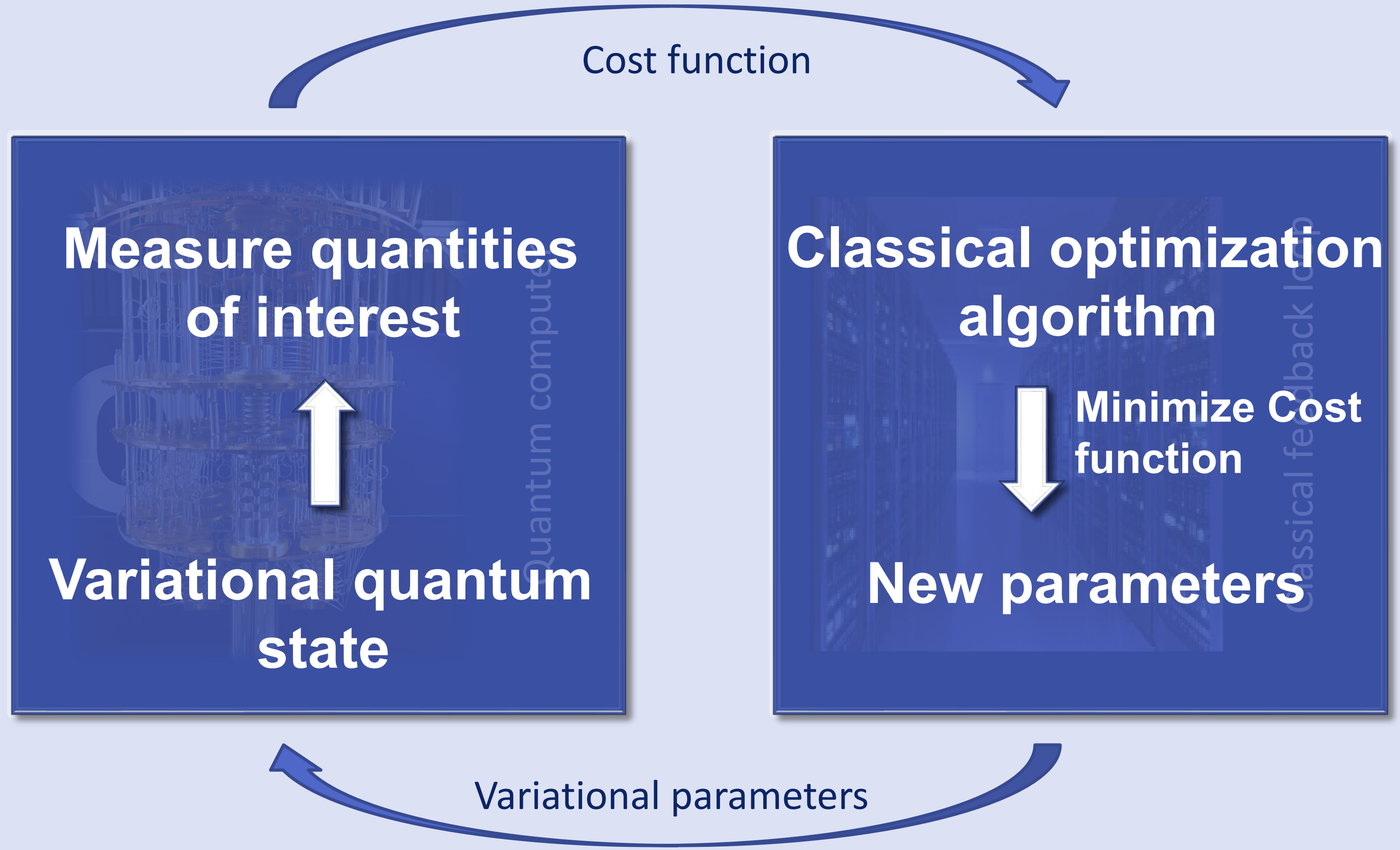

Our work: Extension to **nonlinear** problems

M. Lubasch, J. Joo, P. Moinier, M. Kiffner & DJ, Phys. Rev. A **101**, 010301(R) (2020).

The QNPU Quantum Network for cost function $\mathcal{C}$

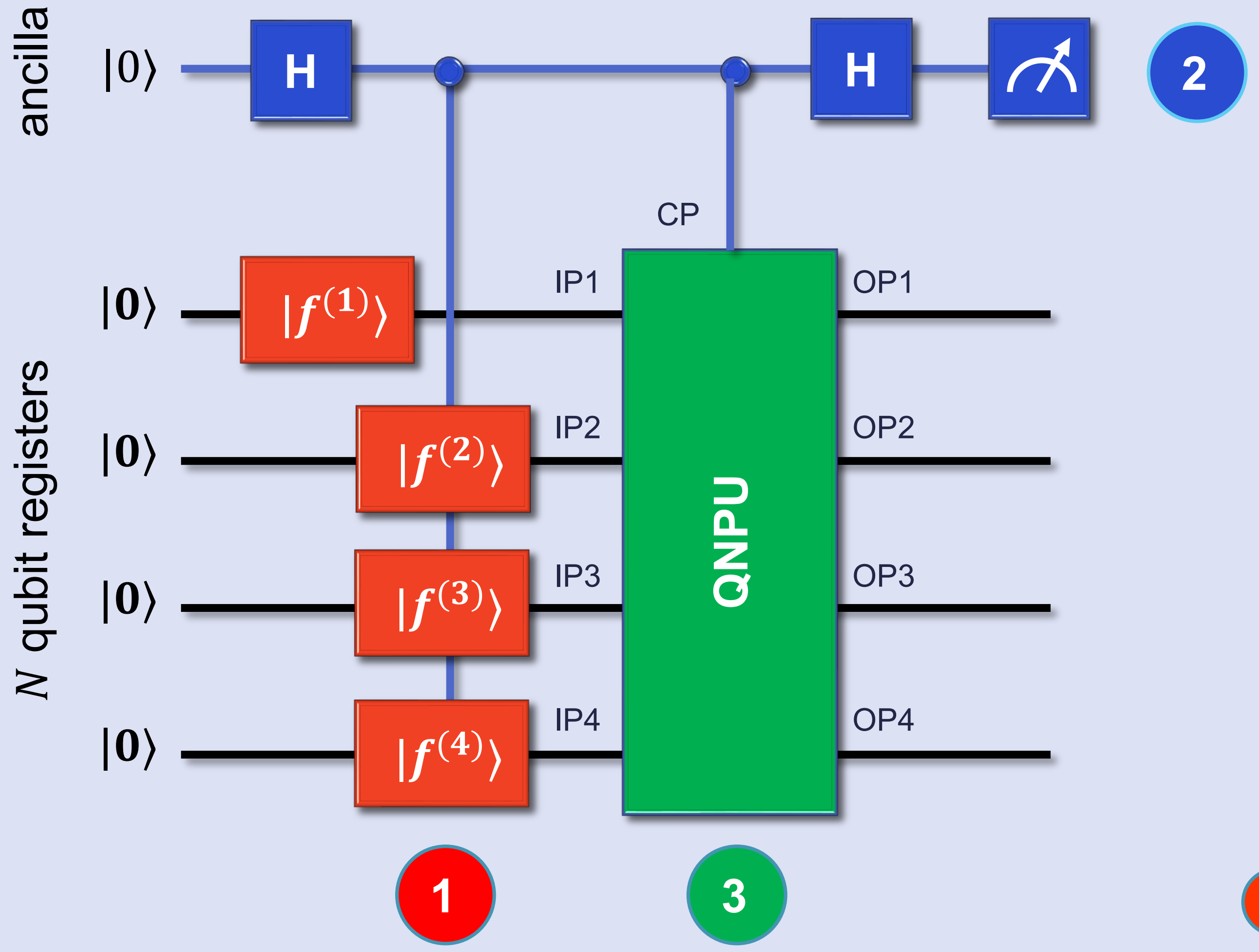

$$\mathcal{C} = f^{(1)^*} \prod_{j=1}^{r} \left(O_j f^{(j)} \right)$$

1. Prepare a variational state ($\propto n$)
2. Measure cost function via ancilla qubit
3. QNPU - evaluate the cost function ($\propto n$)

M. Lubasch, J. Joo, P. Moinier, M. Kiffner & DJ, Phys. Rev. A **101**, 010301(R) (2020).

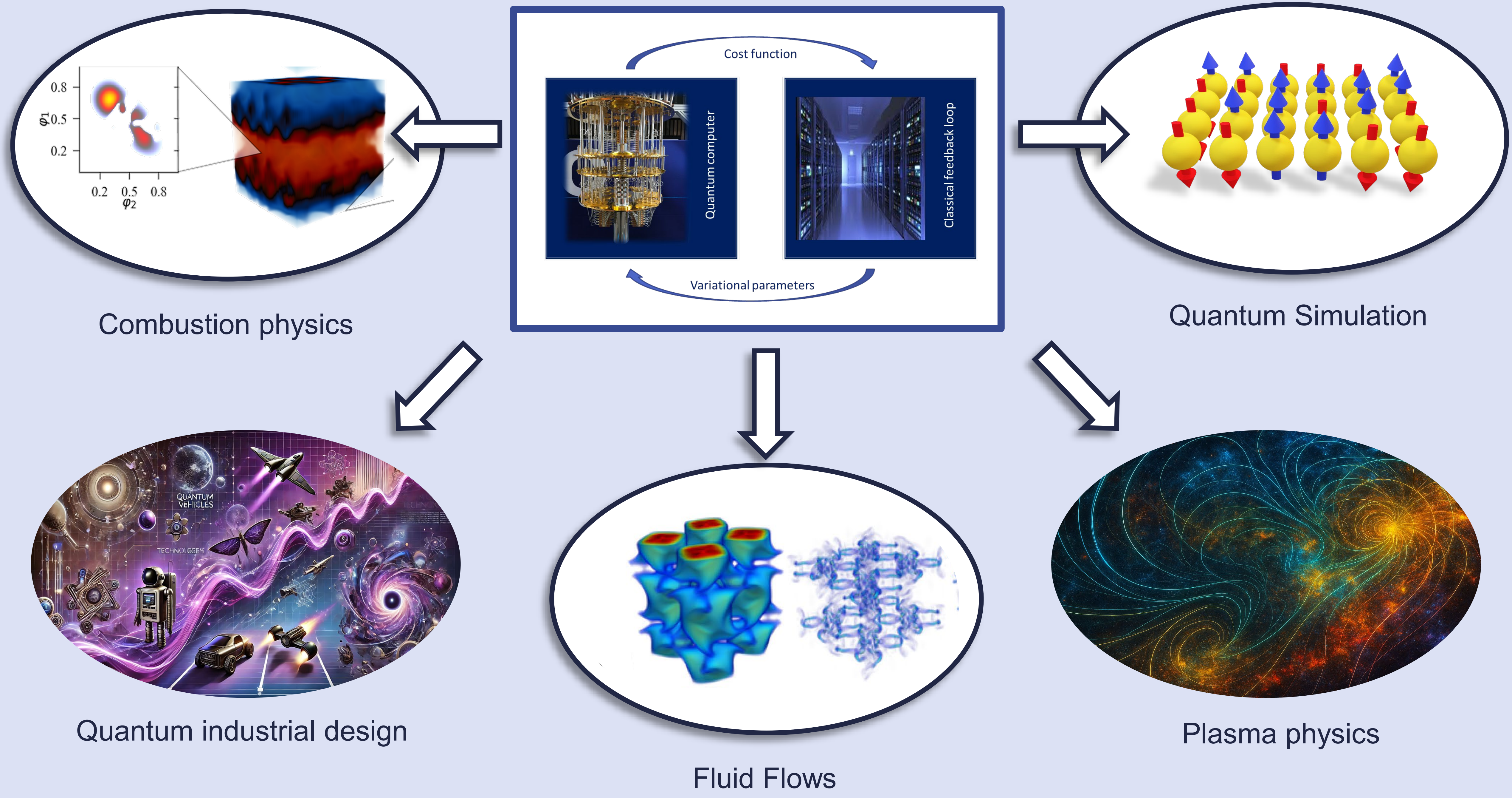
Cost function
Quantum computer
Classical feedback loop
Variational parameters
0.8
φ_1 0.5
0.2
0.2 0.5 0.8
φ_2
Combustion physics
Quantum Simulation
QUANTUM VEHICLES
Quantum industrial design
Fluid Flows
Plasma physics

Tensor networks as a quantum programming paradigm

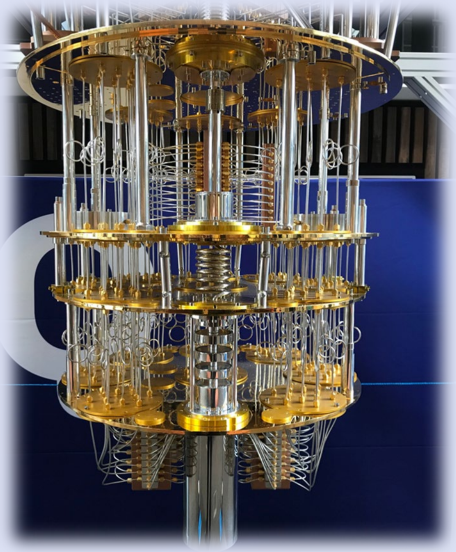

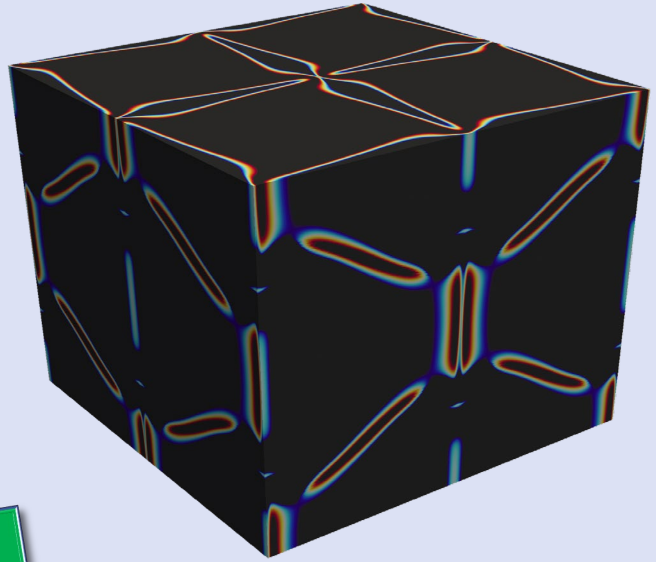

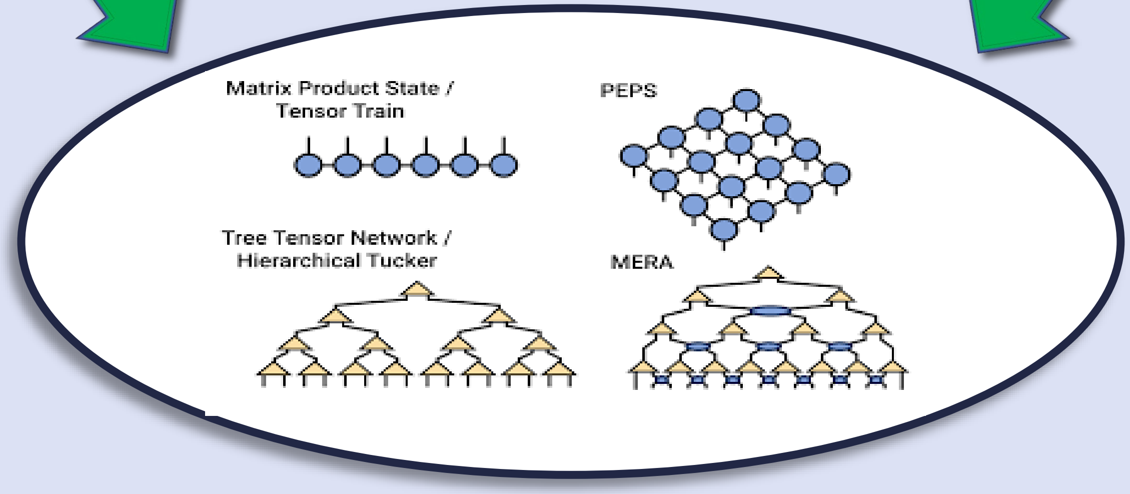

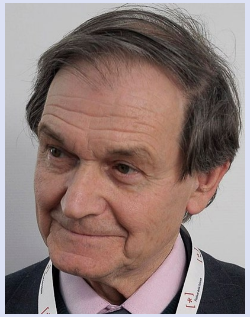

Variational quantum algorithms for computational fluid dynamics,
D Jaksch, P Givi, AJ Daley, T Rung
AIAA journal **61**, 1885 (2023)

Roger Penrose, "Applications of negative dimensional tensors," in Combinatorial Mathematics and its Applications, Academic Press (1971)

❶ Amplitude encoding of discrete functions

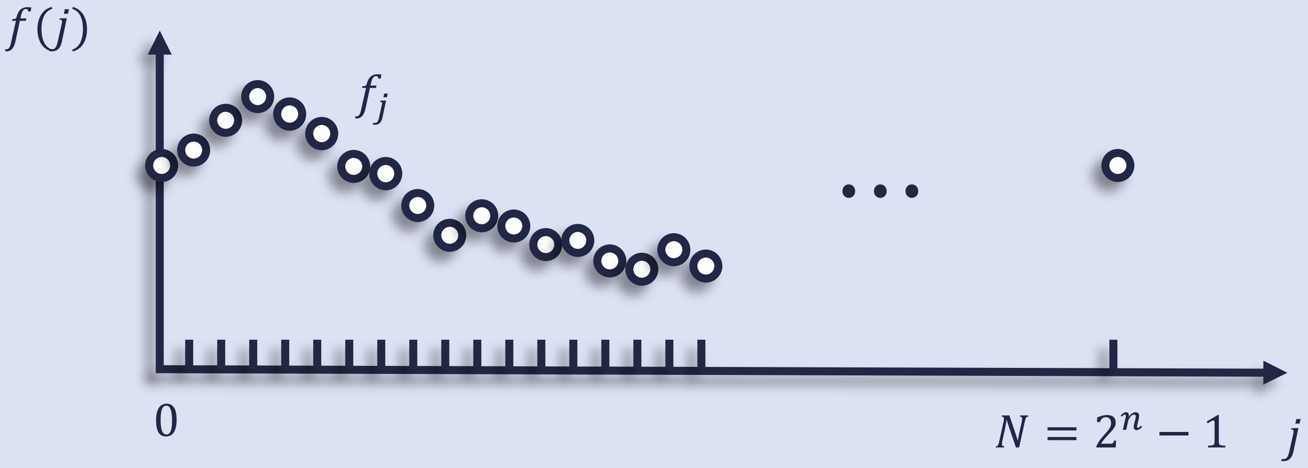

Quantum superposition

$$|\psi\rangle = \sum_i f_i |\vec{\imath}\rangle$$

n-qubit register stores 2^n function values f_j

Map $j \to \vec{\jmath} = \text{binary(j)}$ for $n = 8$:

$j = 0 \to \vec{\jmath} = 00000000$ $\quad$ $j = 1 \to \vec{\jmath} = 00000001$ $\quad$ $j = 2 \to \vec{\jmath} = 00000010$ $\quad$ ... $\quad$ $j = 255 \to \vec{\jmath} = 11111111$

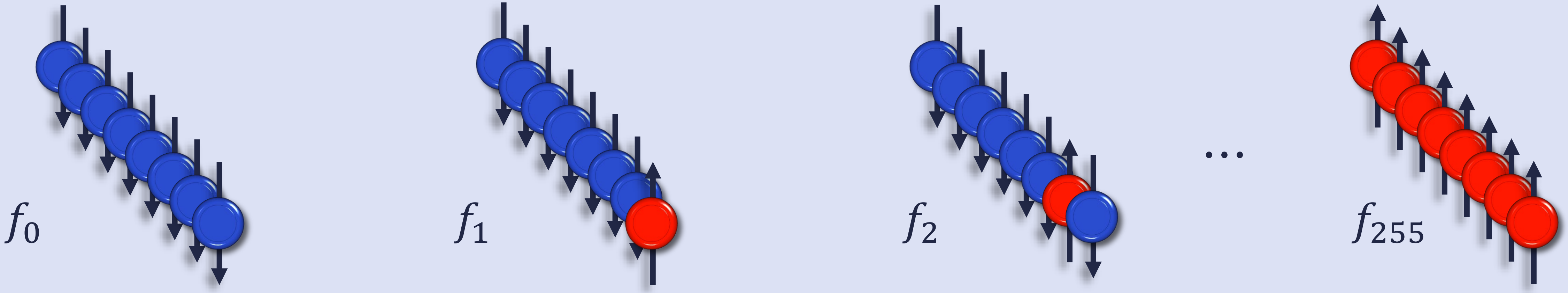

The edge of chaos

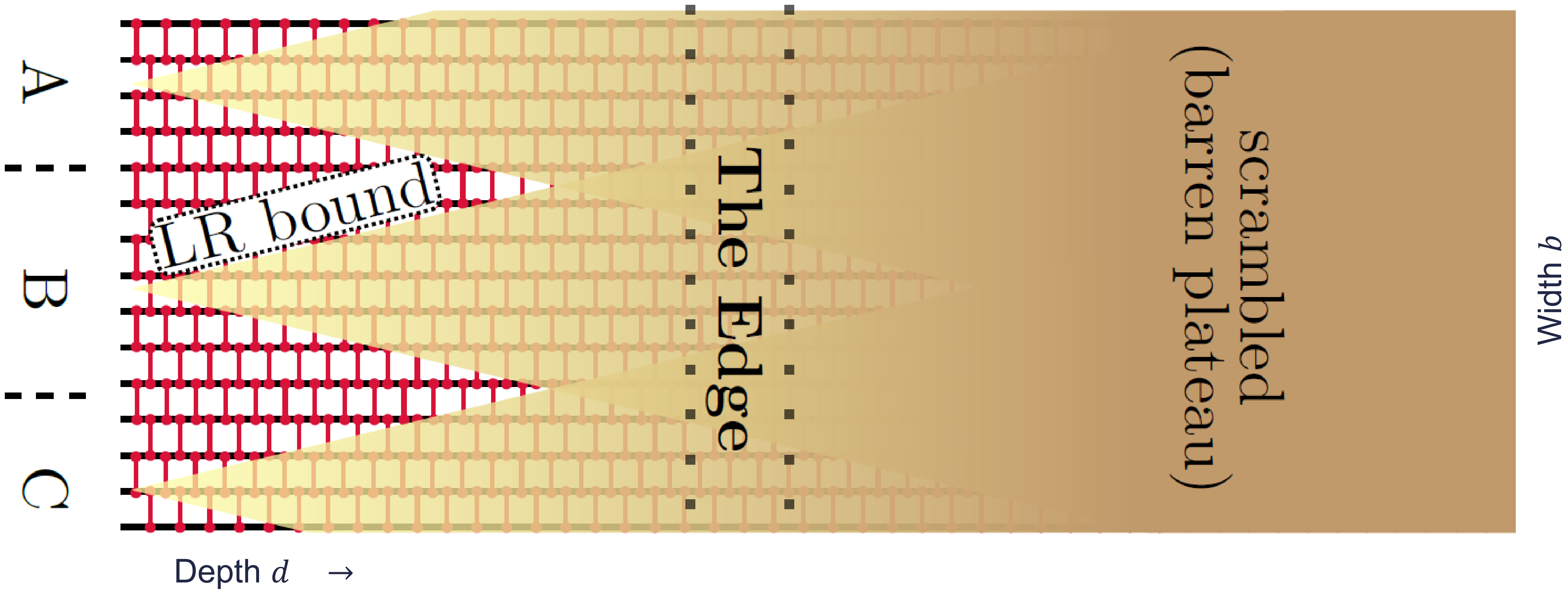

- The Lieb-Robinson bound gives the speed at which effects of gate parameters spread across the system
- When cones overlap the system becomes overdetermined and early gates identical to random circuit

T. Hashizume, et al., *Variational Quantum Computing at the edge of chaos*, in preparation.

Tripartite Mutual Information

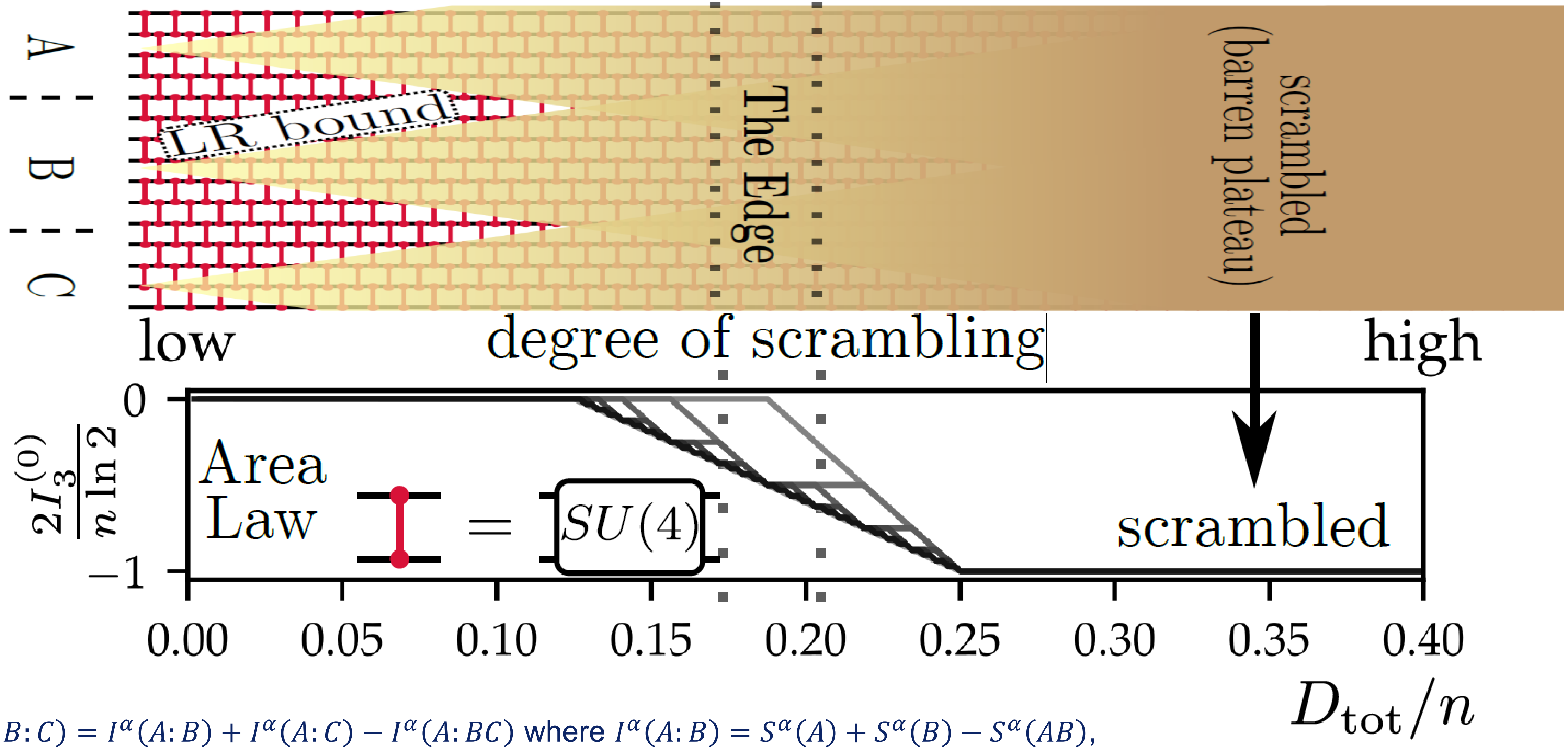

$I_3^\alpha(A:B:C) = I^\alpha(A:B) + I^\alpha(A:C) - I^\alpha(A:BC)$ where $I^\alpha(A:B) = S^\alpha(A) + S^\alpha(B) - S^\alpha(AB)$,
$S^\alpha = \text{tr}(\rho_A^\alpha)/(1-\alpha)$ and $\rho_A = \text{tr}_{\overline{A}}(\rho)$

A quantum Nyquist-Shannon theorem

- We consider an amplitude encoded sin function in n qubits with $x \in [0,1)$ and $k = 2\pi/\lambda$

$$|\psi\rangle = \sum_i \sin(kx_i)|\sigma(i)\rangle$$

- We rewrite this using a tensor train decomposition

$$|\Psi_\lambda\rangle = \sum_{\boldsymbol{\sigma}} \sum_{\boldsymbol{\kappa}} M_{\kappa_0}^{(\sigma_0)} M_{\kappa_0,\kappa_1}^{(\sigma_1)} \ldots M_{\kappa_{n-1}}^{(\sigma_{n-2})} |\boldsymbol{\sigma}\rangle$$

- With tensors

$$M_{\kappa_0}^{(0)} = \begin{pmatrix} \sin\frac{k}{2^n} & \cos\frac{k}{2^n} \end{pmatrix}, M_{\kappa_0}^{(1)} = \begin{pmatrix} 0 & 1 \end{pmatrix} \qquad M_{\kappa_0}^{(0)} = \begin{pmatrix} \cos\frac{k}{2} \\ \sin\frac{k}{2} \end{pmatrix}, M_{\kappa_0}^{(1)} = \begin{pmatrix} 1 & 0 \end{pmatrix}$$

$$M_{\kappa_{q-1},\kappa_q}^{(0)} = \begin{pmatrix} \cos(\frac{k}{2^{n-q}}) & -\sin(\frac{k}{2^{n-q}}) \\ \sin(\frac{k}{2^{n-q}}) & \cos(\frac{k}{2^{n-q}}) \end{pmatrix}, M_{\kappa_{q-1},\kappa_q}^{(1)} = \begin{pmatrix} 1 & 0 \\ 0 & 1 \end{pmatrix}$$

- In the limit $n \to \infty$ we work out the reduced density operator of the q-th qubit

A quantum Nyquist-Shannon theorem

- We obtain for the reduced density operator

$$\rho_q = \lim_{n\to\infty} \sum_{\boldsymbol{\kappa},\boldsymbol{\kappa}',\boldsymbol{\sigma}\neq\sigma_q} M_{\kappa_0}^{(\sigma_0)} \dots M_{\kappa_{n-1}}^{(\sigma_{n-2})} (M_{\kappa'_0}^{(\sigma_0)})^* \dots (M_{\kappa'_{n-1}}^{(\sigma_{n-2})})^*$$

$$= \begin{pmatrix} \frac{2k - \sec(2^{-q-1}k)\sin((2+2^{-q-1})k) + \tan 2^{-q-1}k}{4k - 2\sin 2k} & \frac{2k\cos 2^{-q-1}k - \frac{\sin 2k}{\cos 2^{-q-1}k}}{(4k - 2\sin 2k)} \\ \frac{2k\cos 2^{-q-1}k - \frac{\sin 2k}{\cos 2^{-q-1}k}}{(4k - 2\sin 2k)} & \frac{2k - \sec(2^{-q-1}k)\sin((2-2^{-q-1})k) - \tan 2^{-q-1}k}{4k - 2\sin 2k} \end{pmatrix}$$

- This density operator converges to

$$\lim_{q\to\infty} \rho_q = |+\rangle_q\langle+|$$

- exponentially with q for $q > q_c(\lambda)$ with

$$q_c(\lambda) = \log_2\left(\frac{\pi}{\lambda}\right)$$

- A qubit state $|+\rangle_q\langle+|$ corresponds to linear interpolation and hence only q_c qubits are required in the TT.

Example: The Weierstrass function

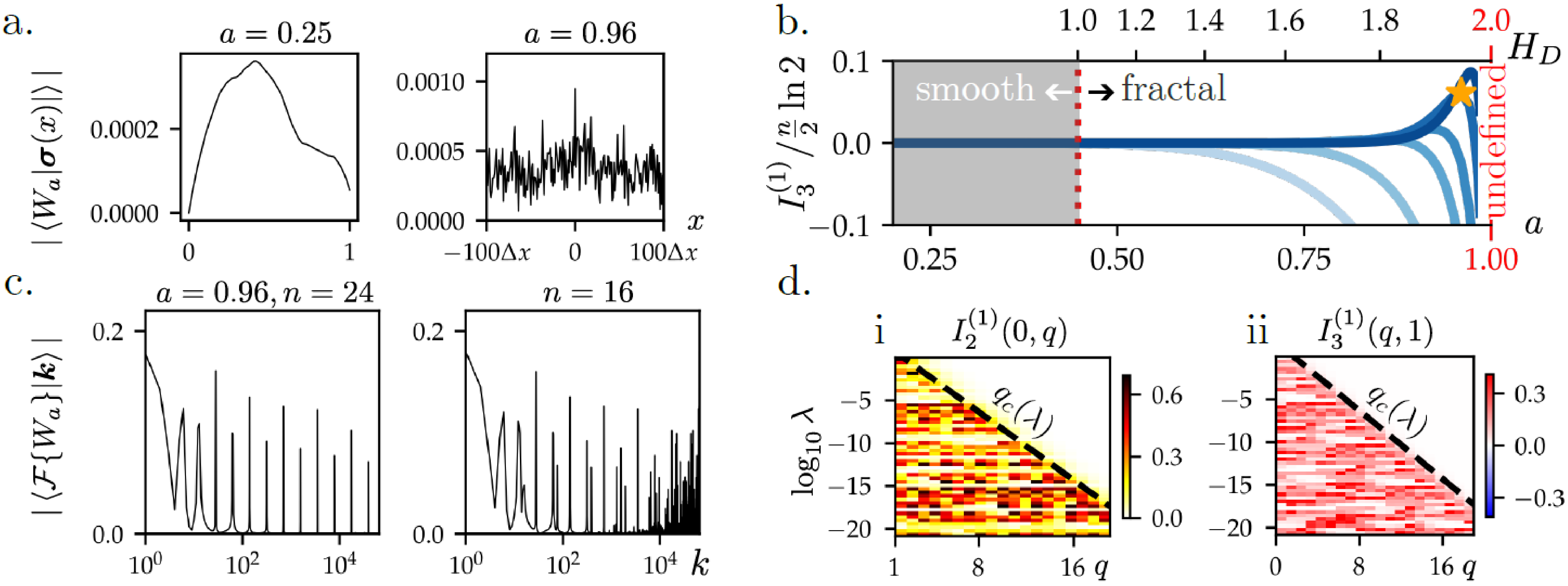

Weierstrass $W(x) = \sum_n a^n \sin(b^n \pi x)$, smooth for $a < \frac{1}{b}$ and fractal for $\frac{1}{b} < a < 1$. Here for $b = \sqrt{5}$.

Trainability and Tripartite Mutual Information

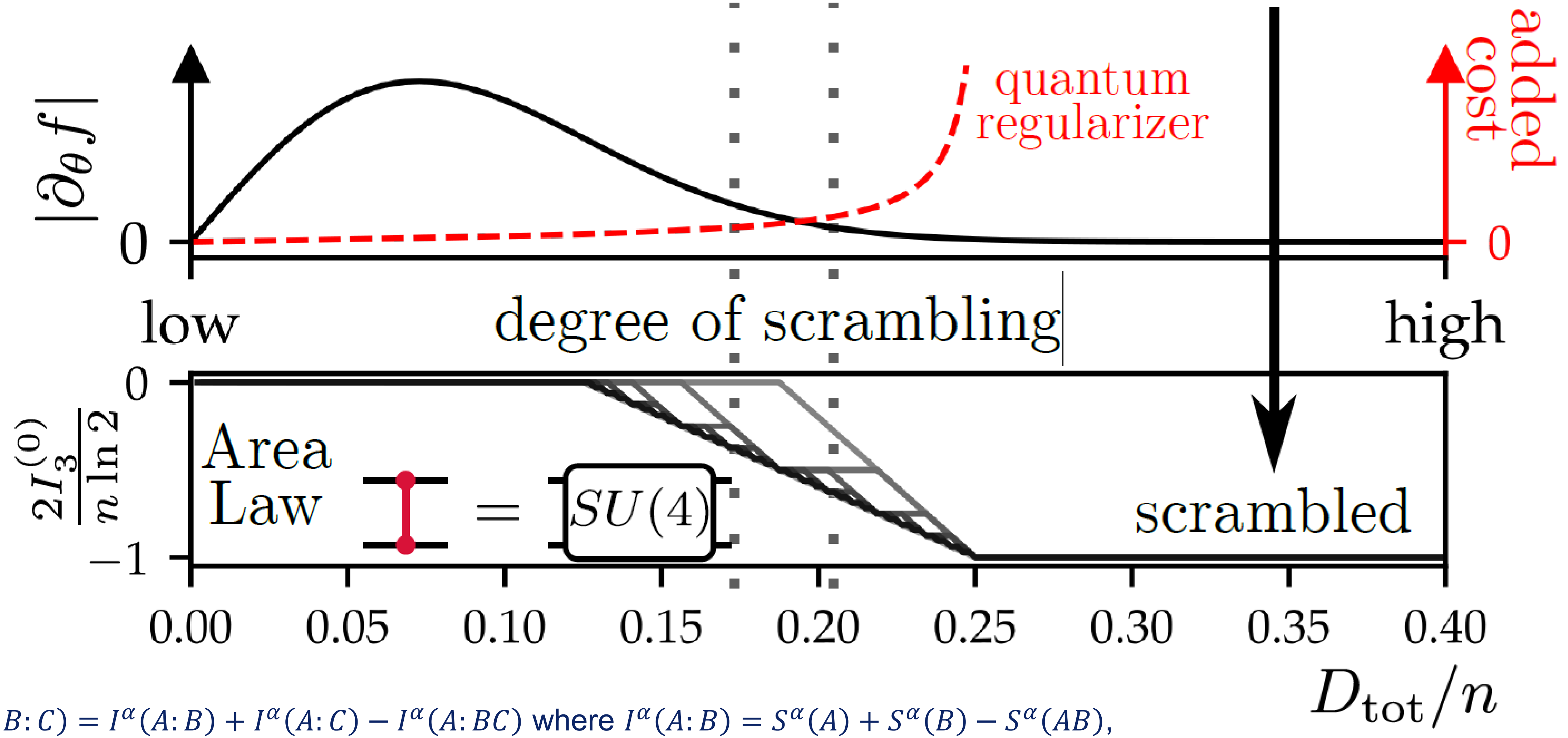

$I_3^\alpha(A{:}B{:}C) = I^\alpha(A{:}B) + I^\alpha(A{:}C) - I^\alpha(A{:}BC)$ where $I^\alpha(A{:}B) = S^\alpha(A) + S^\alpha(B) - S^\alpha(AB)$,
$S^\alpha = \mathrm{tr}(\rho_A^\alpha)/(1-\alpha)$ and $\rho_A = \mathrm{tr}_{\bar{A}}(\rho)$

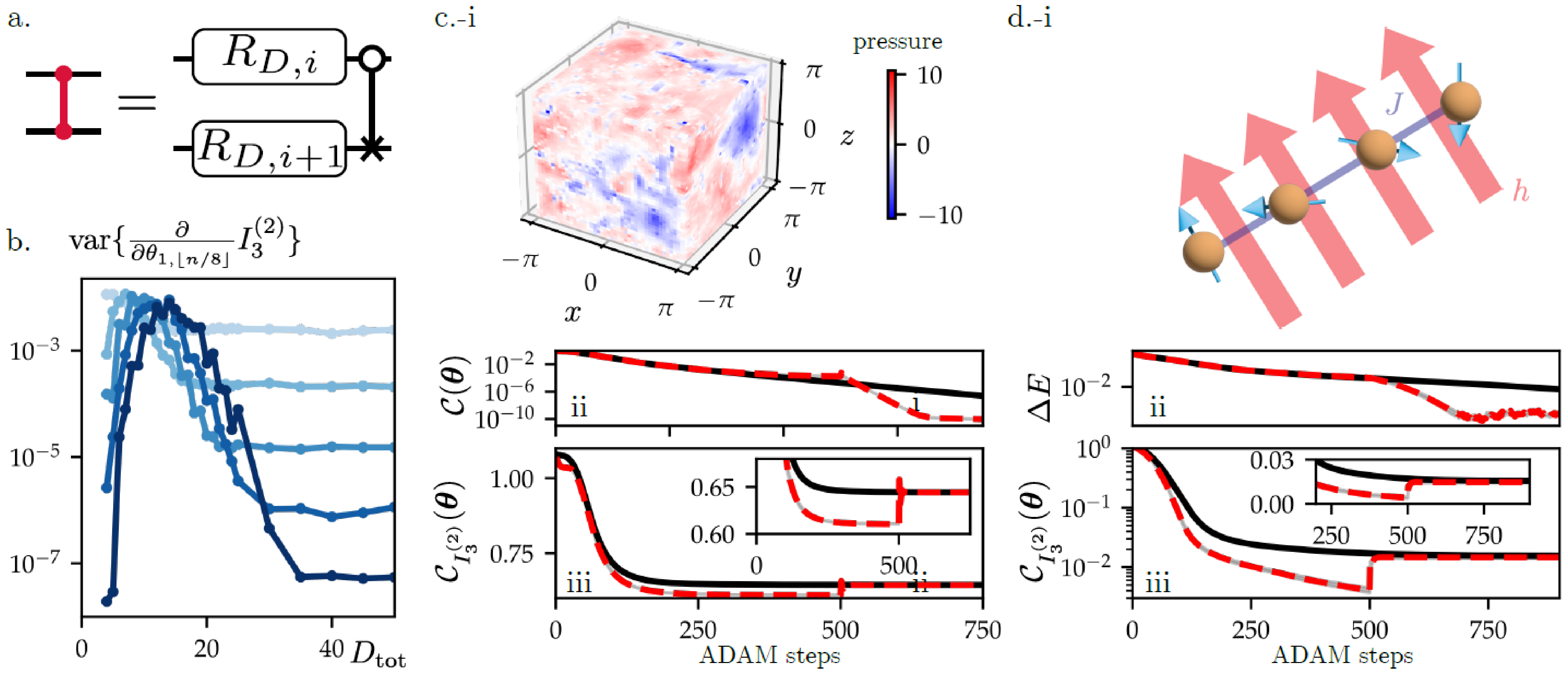

a.
$R_{D,i}$
$R_{D,i+1}$
b.
$\mathrm{var}\{\frac{\partial}{\partial\theta_{1,\lfloor n/8\rfloor}} I_3^{(2)}\}$
10^{-3}
10^{-5}
10^{-7}
0
20
40 D_{tot}
c.-i
pressure
10
0
−10
π
0
z
$-\pi$
π
0
y
$-\pi$
$-\pi$
0
x
π
$\mathcal{C}(\boldsymbol{\theta})$
10^{-2}
10^{-6}
10^{-10}
ii
$\mathcal{C}_{I_3^{(2)}}(\boldsymbol{\theta})$
1.00
0.75
0.65
0.60
0
500
iii
0
250
500
750
ADAM steps
d.-i
J
h
ΔE
10^{-2}
ii
$\mathcal{C}_{I_3^{(2)}}(\boldsymbol{\theta})$
10^{0}
10^{-1}
10^{-2}
0.03
0.00
250
500
750
iii
0
250
500
750
ADAM steps

Modified Variational Quantum Algorithm

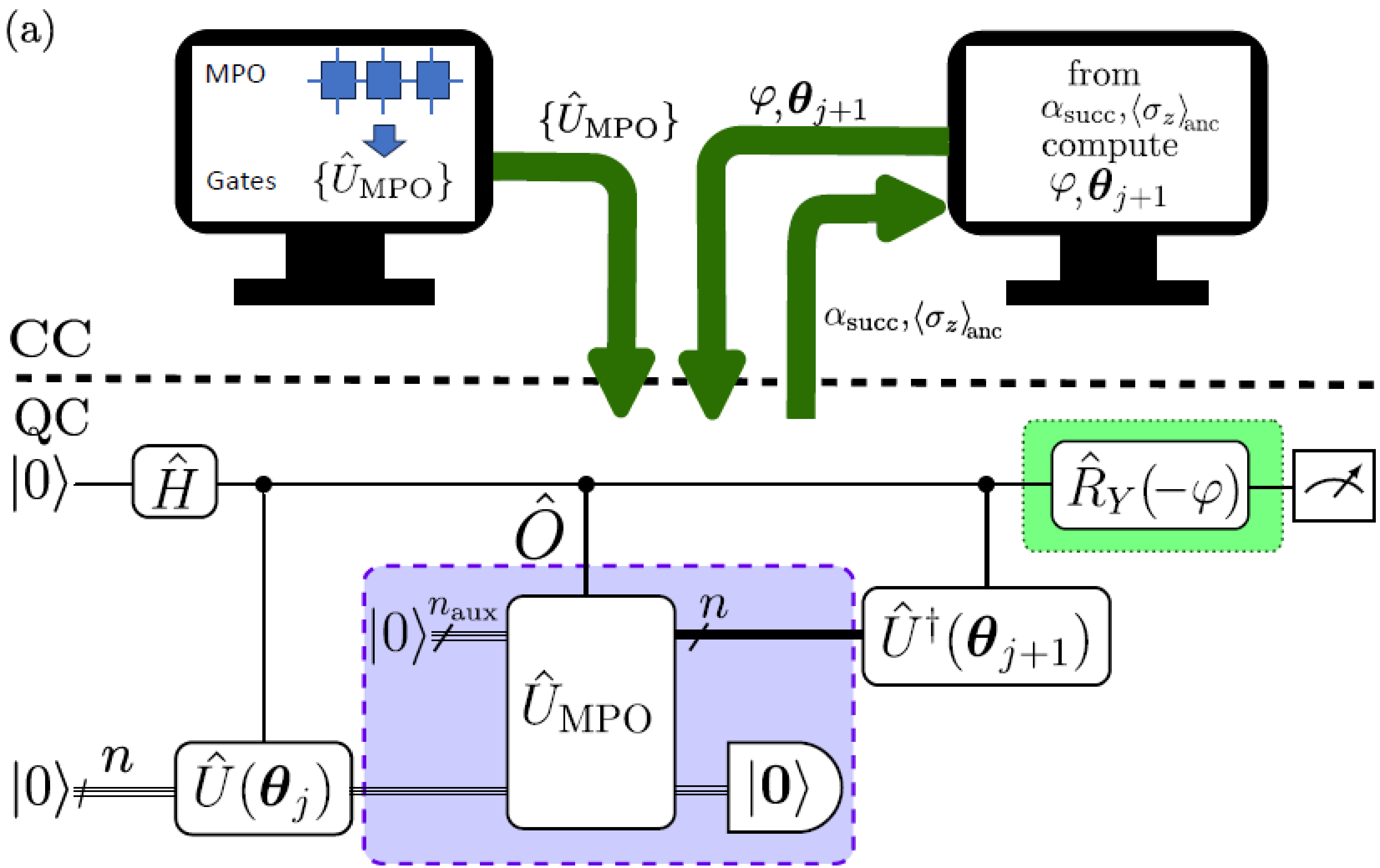

Termanova, et al., *Tensor quantum programming*, New J. Phys. **26**, 123019 (2024).

P. Siegl et al., Tensor-Programmable Quantum Circuits for Solving Differential Equations, arXiv:2502.04425.

Optimizing for a nonlinear term in PDEs

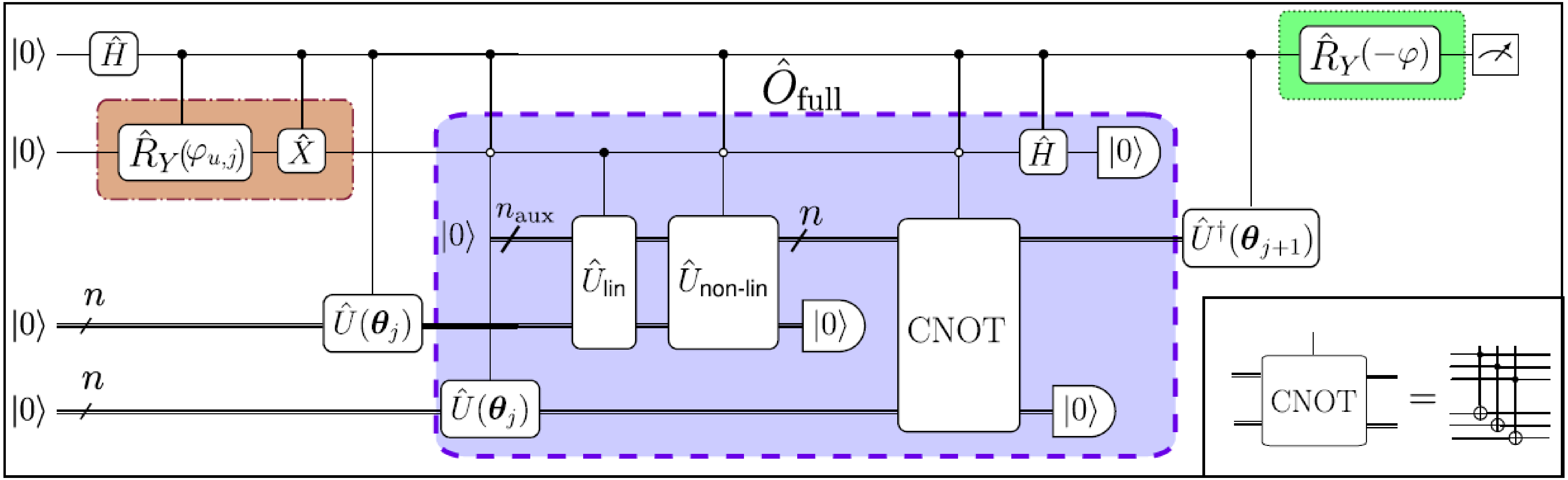

P. Siegl et al., Tensor-Programmable Quantum Circuits for Solving Differential Equations, arXiv:2502.04425.

Example: Incompressible Flow

Incompressible Navier-Stokes equation

- We solve the 2D and 3D equations for simple fluid flows

$$\frac{\partial \vec{v}}{\partial t} = -(\vec{v} \cdot \nabla)\vec{v} - \nabla p + \frac{1}{\mathrm{Re}} \nabla^2 \vec{v}$$

$$\nabla \cdot \vec{v} = 0$$

- 2D → weather forecast
- 3D → aerodynamics, combustion physics, …

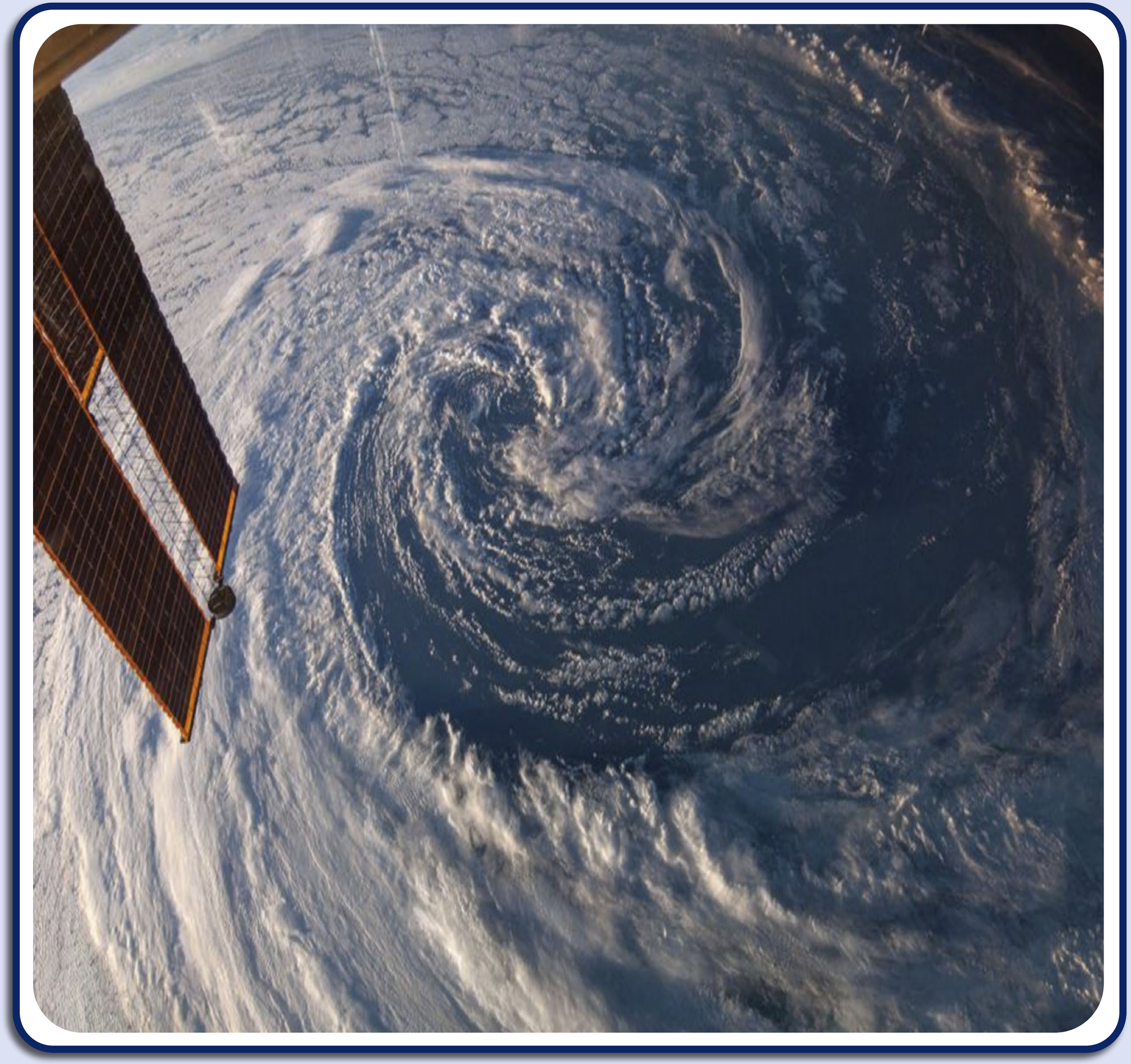

Kolmogorov microscale and Reynolds number

- A simulation of fluid flow needs to cover a wide range of length scales
  - L the size of the largest eddies in the flow
  - η the Kolmogorov length scale at which eddies are dissipated into heat
- The ratio of these two length scales is the Reynolds number defined as

$$\mathrm{Re} = \left(\frac{L}{\eta}\right)^{4/3} = \frac{vL}{\nu}$$

- Here v is the speed of the flow and ν the kinematic viscosity
- Flows become turbulent when Re is greater than a couple of thousands
- Grid based methods typically scale with $\mathrm{Re}^{3K/4}$

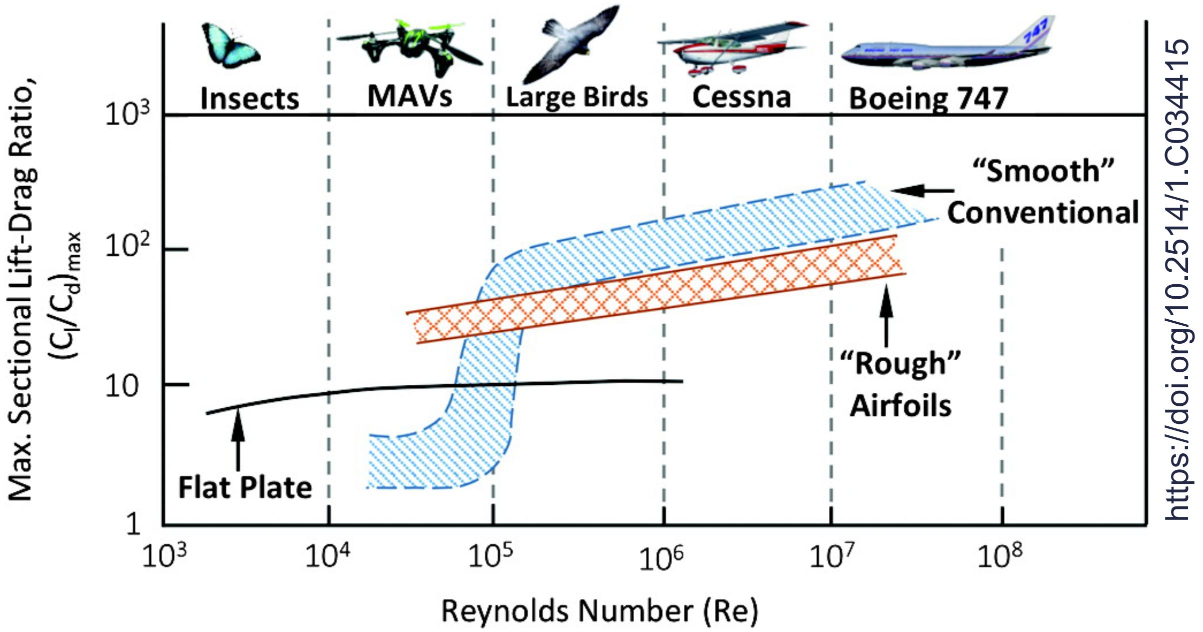

wikipedia

$\mathrm{Re} \approx 10^9$

newscientist.com

$\mathrm{Re} \approx$ very large

MPS algorithm for evolving a 2D fluid flow in time

- We illustrate this by considering a simple Euler step to move forward in time by Δt.
- For this we minimize the cost function

$$\Theta(\vec{v}^*) = \mu|\bar{\nabla}\cdot\vec{v}^*|^2 + \left|\frac{\vec{v}^* - \vec{v}}{\Delta t} + (\vec{v}\cdot\bar{\nabla})\vec{v} - \nu\bar{\nabla}^2\vec{v}\right|^2$$

- We use eighth-order central finite difference stencils and represent the Laplace operator as an MPO.
- We write out explicitly $\vec{v} = u_1\vec{e}_1 + u_2\vec{e}_2$ and $\vec{v}^* = u_1^*\vec{e}_1 + u_2^*\vec{e}_2$ and write the components as bold vectors on the grid, e.g. $\boldsymbol{u}_1 = \{u_1(r_1), u_1(r_1)\cdots\}$ and rewrite the cost function as

$$\Theta(\boldsymbol{V}^*) = \sum_{i,j=1}^{2}\left\{\mu\left(\frac{\Delta\boldsymbol{u}_i^*}{\Delta x_i}\right)^t\frac{\Delta\boldsymbol{u}_j^*}{\Delta x_j}\right\} + \sum_{i=1}^{2}\left\{\frac{(\boldsymbol{u}_i^*)^t\boldsymbol{u}_i^*}{\Delta t^2} + \frac{(\boldsymbol{u}_i^*)^t}{\Delta t}\left(\frac{-\boldsymbol{u}_i}{\Delta t} + \sum_{j=1}^{2}\left\{\boldsymbol{u}_j\frac{\Delta\boldsymbol{u}_i}{\Delta x_j} - \nu\frac{\Delta^2\boldsymbol{u}_i}{\Delta x_j^2}\right\}\right)\right.$$
$$\left. + \left(\frac{-\boldsymbol{u}_i}{\Delta t} + \sum_{j=1}^{2}\left\{\boldsymbol{u}_j\frac{\Delta\boldsymbol{u}_i}{\Delta x_j} - \nu\frac{\Delta^2\boldsymbol{u}_i}{\Delta x_j^2}\right\}\right)^t\frac{\boldsymbol{u}_i^*}{\Delta t}\right\} + \left[\ldots\right],$$

- The terms in $[\cdots]$ are constant and thus irrelevant for the optimization, a step scales like $\mathcal{O}(N\chi^4)$ or $\mathcal{O}(\chi^4\log L)$.

CFD Examples – Jet Formation

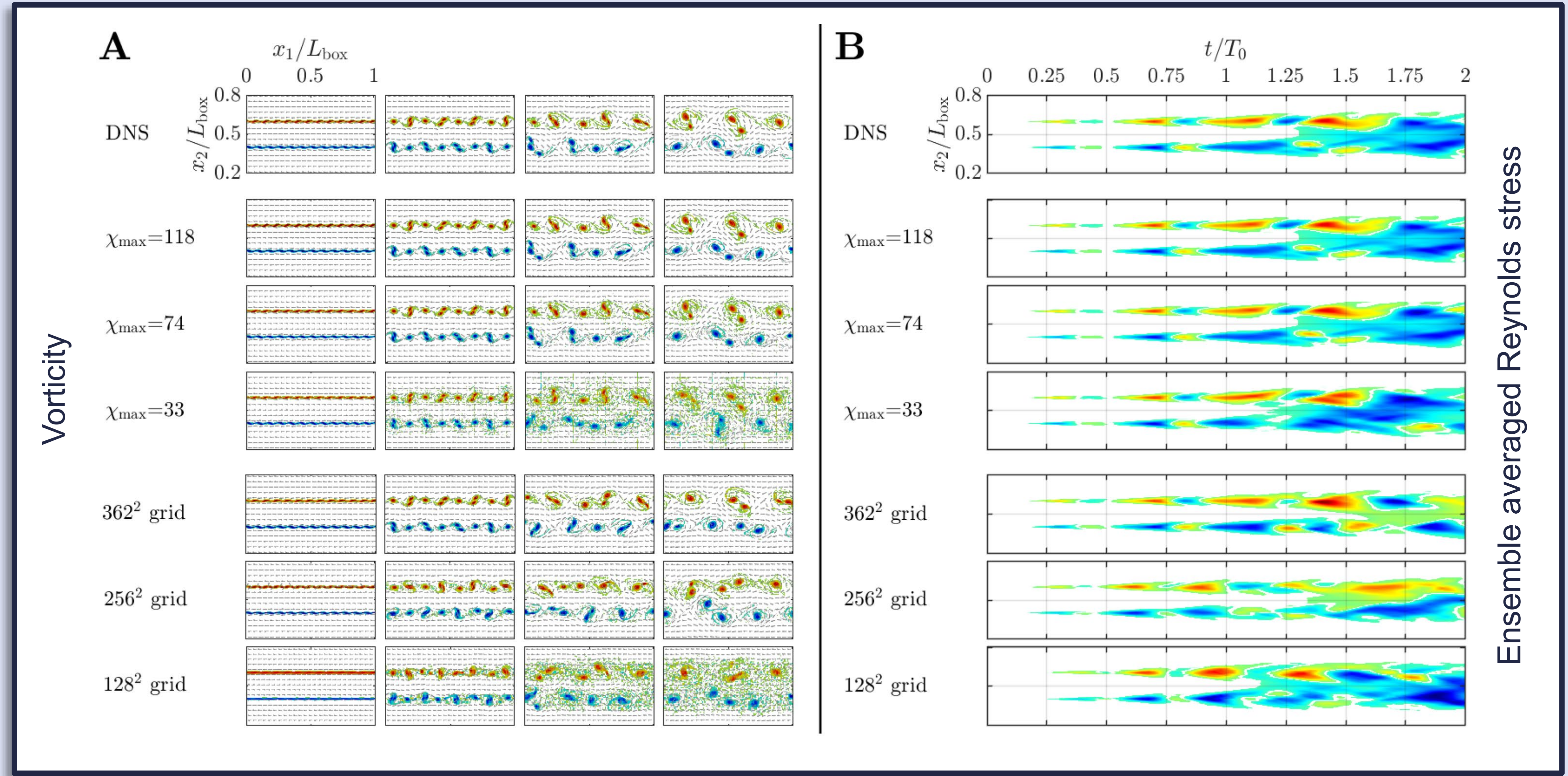

N. Gourianov, et al., Nature Computational Science **2**, 30 (2022).

CFD Examples – Jet Formation

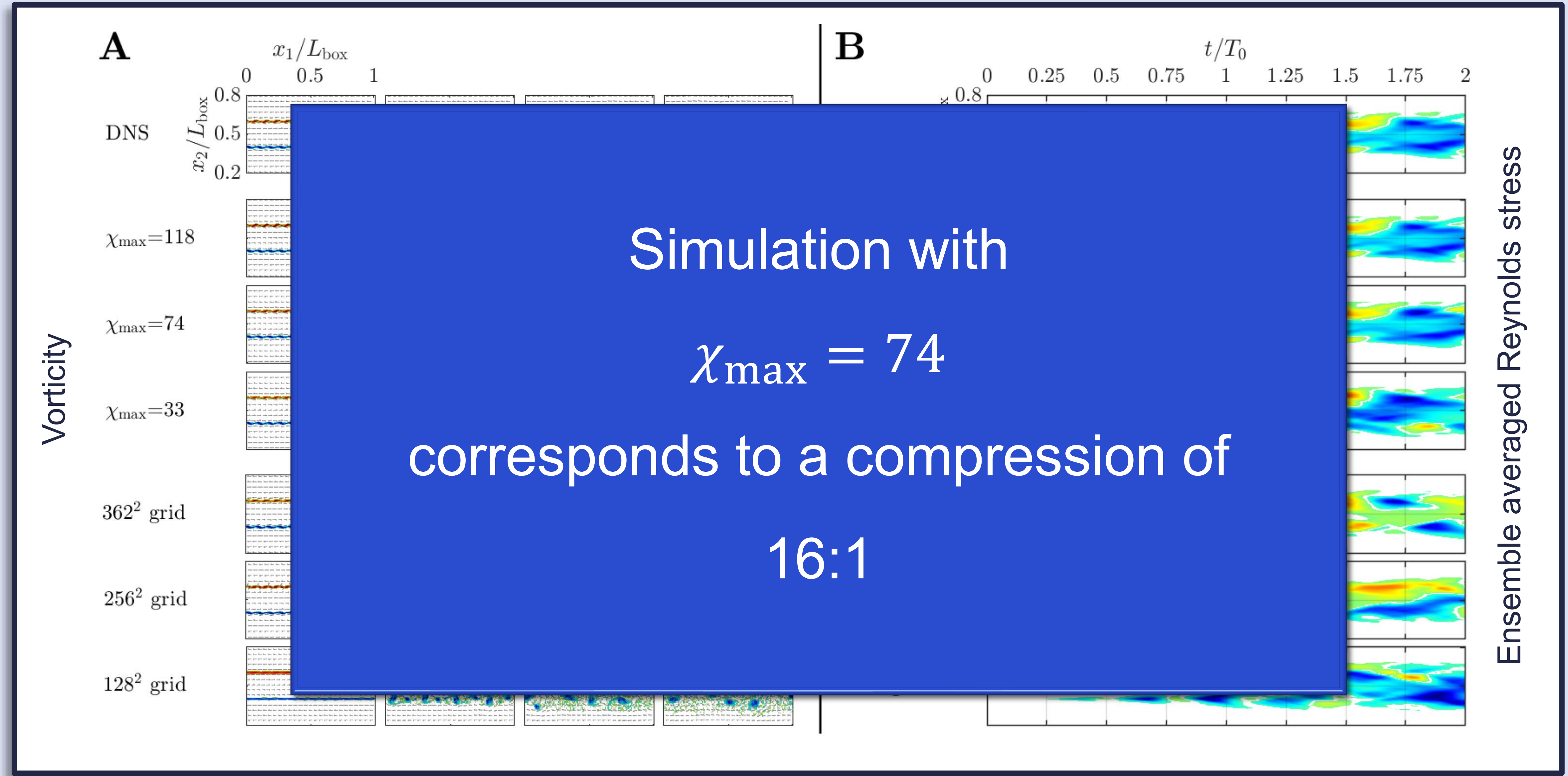

Simulation with

$\chi_{\max} = 74$

corresponds to a compression of

16:1

N. Gourianov, et al., Nature Computational Science **2**, 30 (2022).

Example: Magnus Effect

Body fitted coordinates – flow around a cylinder

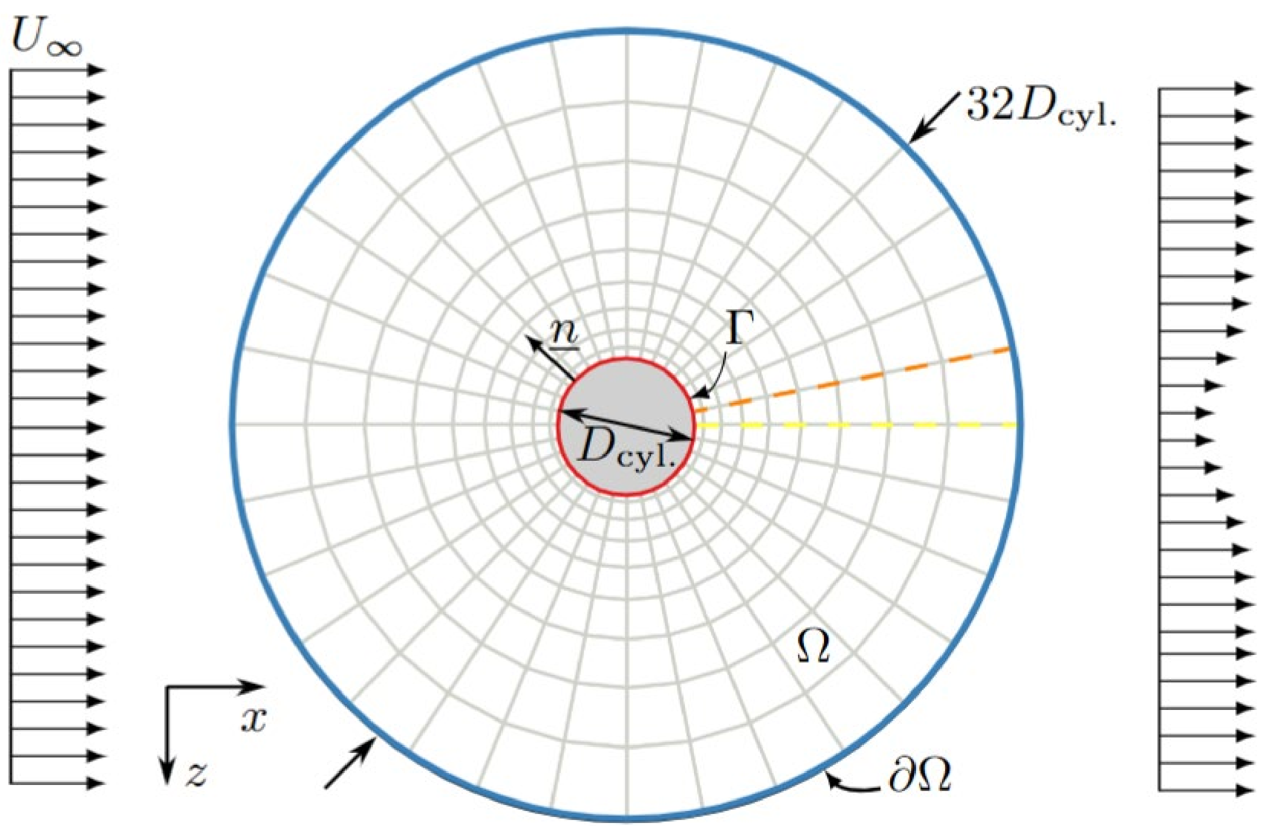

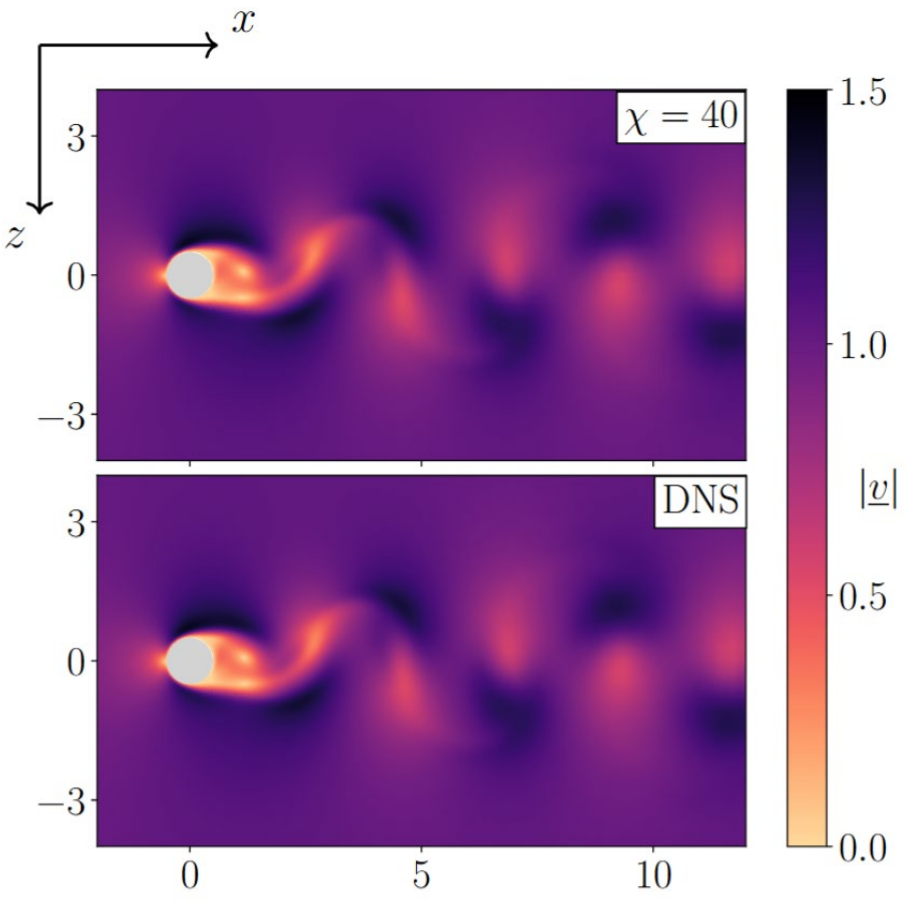

- Generate a body-fitted mesh from a one-dimensional boundary point distribution for convex objects.
- Transform cartesian differential operators into curvilinear matrix product operators, using a given set of grid coordinates.
- Compute key flow characteristics, such as aerodynamic lift and drag coefficients and use to benchmark computations

Body fitted coordinates – flow around a cylinder

- Lift coefficient C_L

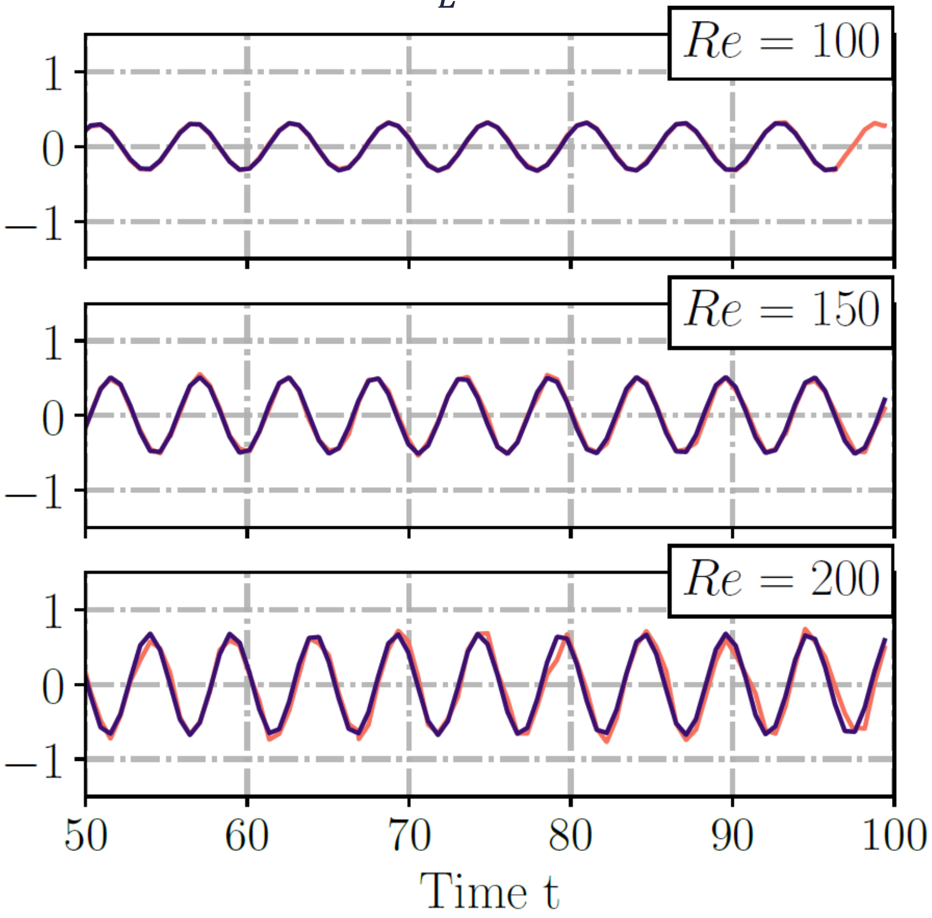

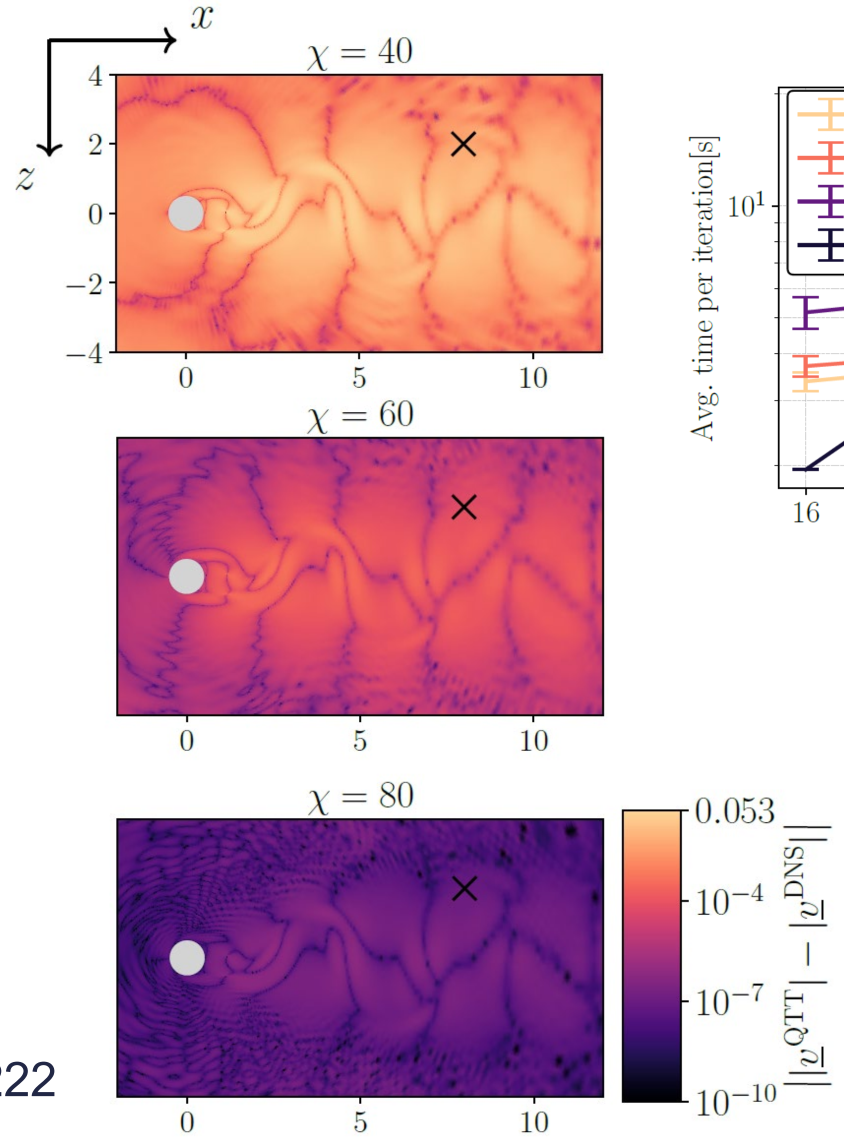

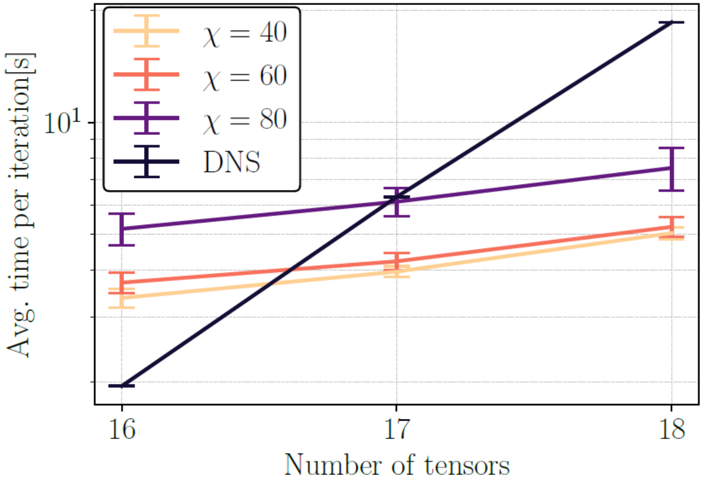

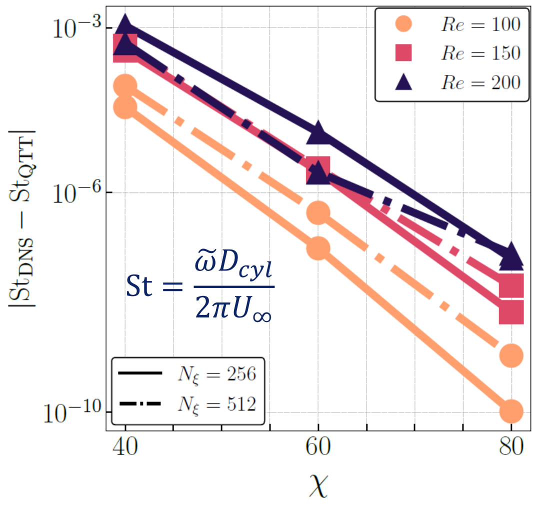

Nis-Luca van Huelst et al., arXiv:2507.05222

Body fitted coordinates – Magnus effect

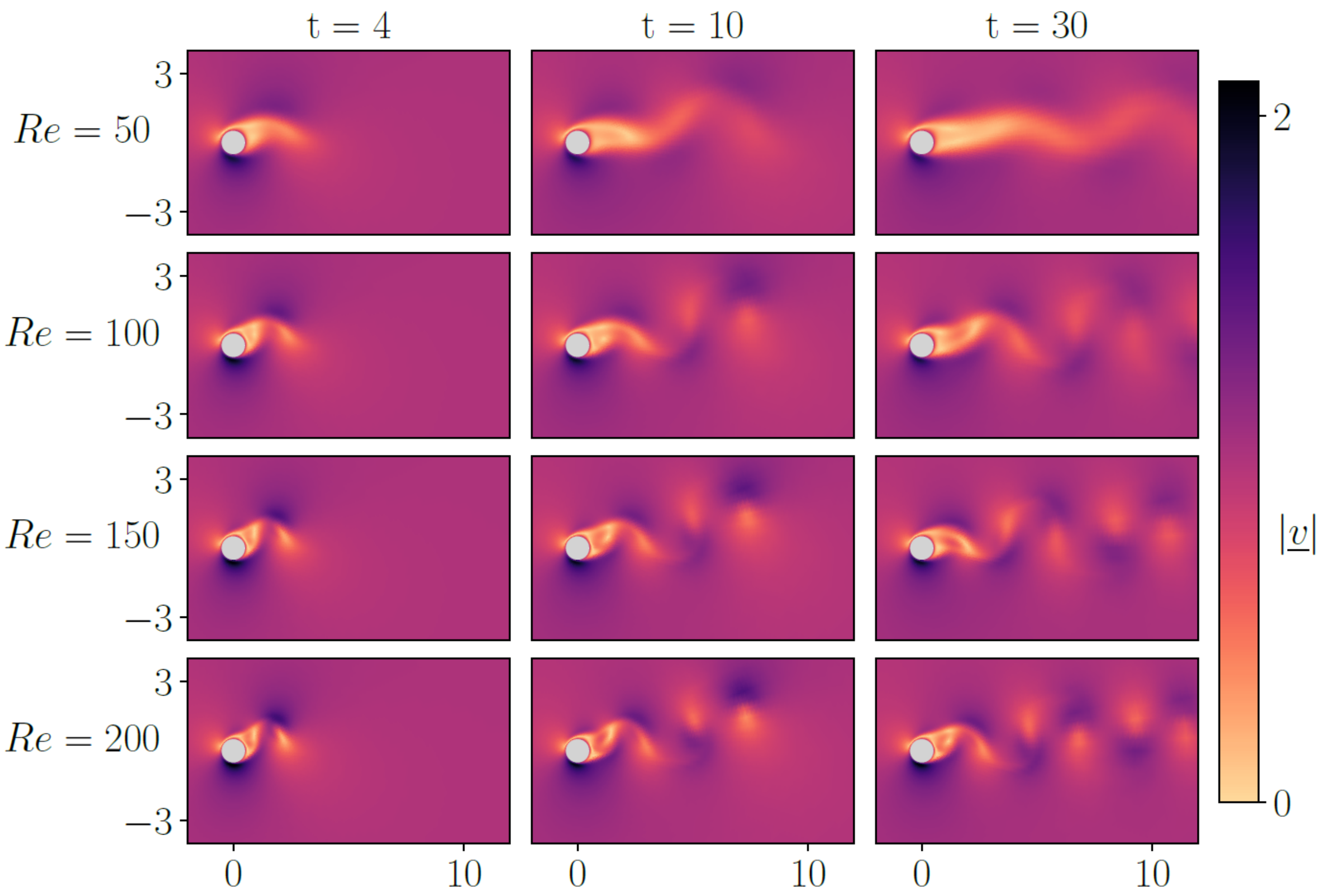

Nis-Luca van Huelst et al., arXiv:2507.05222 (2025)

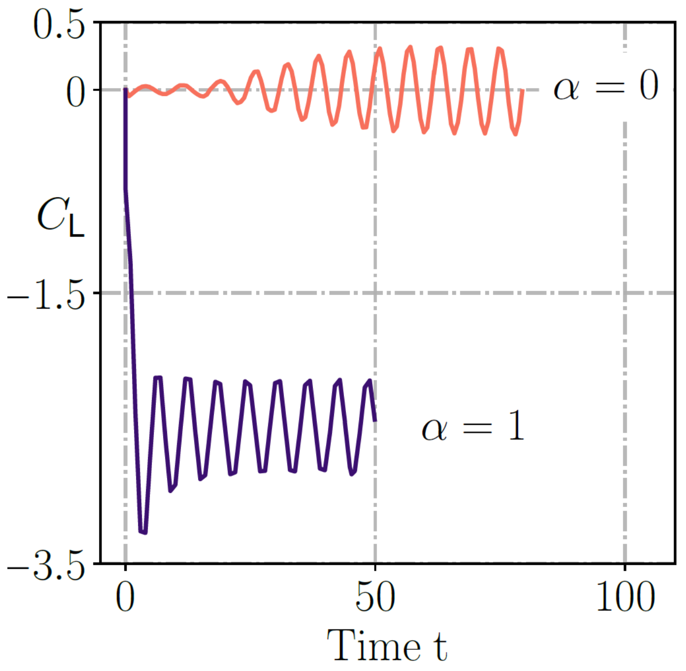

Tangental velocity $U_T = \alpha U\_\infty$

Discretization	χ	$\overline{C}_L$ abs	$\overline{C}_L$ %	St abs	St %
241 × 241	–	**2.4881**	-	**0.1655**	–
258 × 256	40	2.4914	0.13	0.1662	0.40
258 × 256	50	2.4899	0.07	0.1663	0.48
258 × 256	60	2.4904	0.09	0.1663	0.47

Example: Combustive Flow

Probability density function (PDF) for turbulent flows

- The flow is studied in terms of a PDF

$$f = f(\boldsymbol{u}, \varphi_1, \cdots; \boldsymbol{x}, t)$$

across space x and time t.

- The quantites $\boldsymbol{u}, \varphi_1$ are sample space variables of the velocity field and e.g. mass fraction.
- Here, for simplicity we consider a fixed velocity field that is set to be a jet flow combined with a Taylor-Green vortex.
- For a two species flow we then write

$$f = f(\varphi_1, \varphi_2; \boldsymbol{x}, t)$$

- The mean mass fraction is then given by

$$\langle \Phi_\alpha \rangle(\boldsymbol{x}, t) = \int \varphi_\alpha f(\varphi_1, \varphi_2; \boldsymbol{x}, t) \mathrm{d}\varphi_1 \mathrm{d}\varphi_2$$

- Deriving the equation governing f requires sub-grid scale SGS closure modelling.
- We use the Smagorinsky closure

$$\gamma_{\mathrm{SGS}} = C_s \frac{\Delta_\ell^2}{2} \sqrt{\sum_{ij} \left(\frac{\partial U_i}{\partial x_j} + \frac{\partial U_j}{\partial x_i} \right)^2}$$

- Here C_s is an empirical constant and Δl the LES filter width.
- Scalar mixing from SGS turbulence and is modeled by the least-mean-square estimation closure giving

$$\Omega_{\mathrm{mix}} = C_\Omega \frac{\gamma + \gamma_{\mathrm{SGS}}}{\Delta_\ell^2}$$

Fokker-Planck equation

$$\frac{\partial f}{\partial t} + \langle U_i \rangle \frac{\partial f}{\partial x_i} - \frac{\partial}{\partial x_i}\left[(\gamma + \gamma_{\mathrm{SGS}})\frac{\partial f}{\partial x_i}\right] = \frac{\partial}{\partial \varphi_\alpha}\left[\Omega_{\mathrm{mix}}\left(\varphi_\alpha - \langle \Phi_\alpha \rangle\right) f\right] - \frac{\partial}{\partial \varphi_\alpha}(S_\alpha f)$$

Here we have

$$S_1 = S_2 = -\,C_r \varphi_1 \varphi_2$$

where C_r denotes the reaction rate that defines the Damköhler number

$$\mathrm{Da} = C_r l_0 / u_0$$

where l_0 and u_0 are the typical length and velocity scales.

LES Simulation – stochastic closure

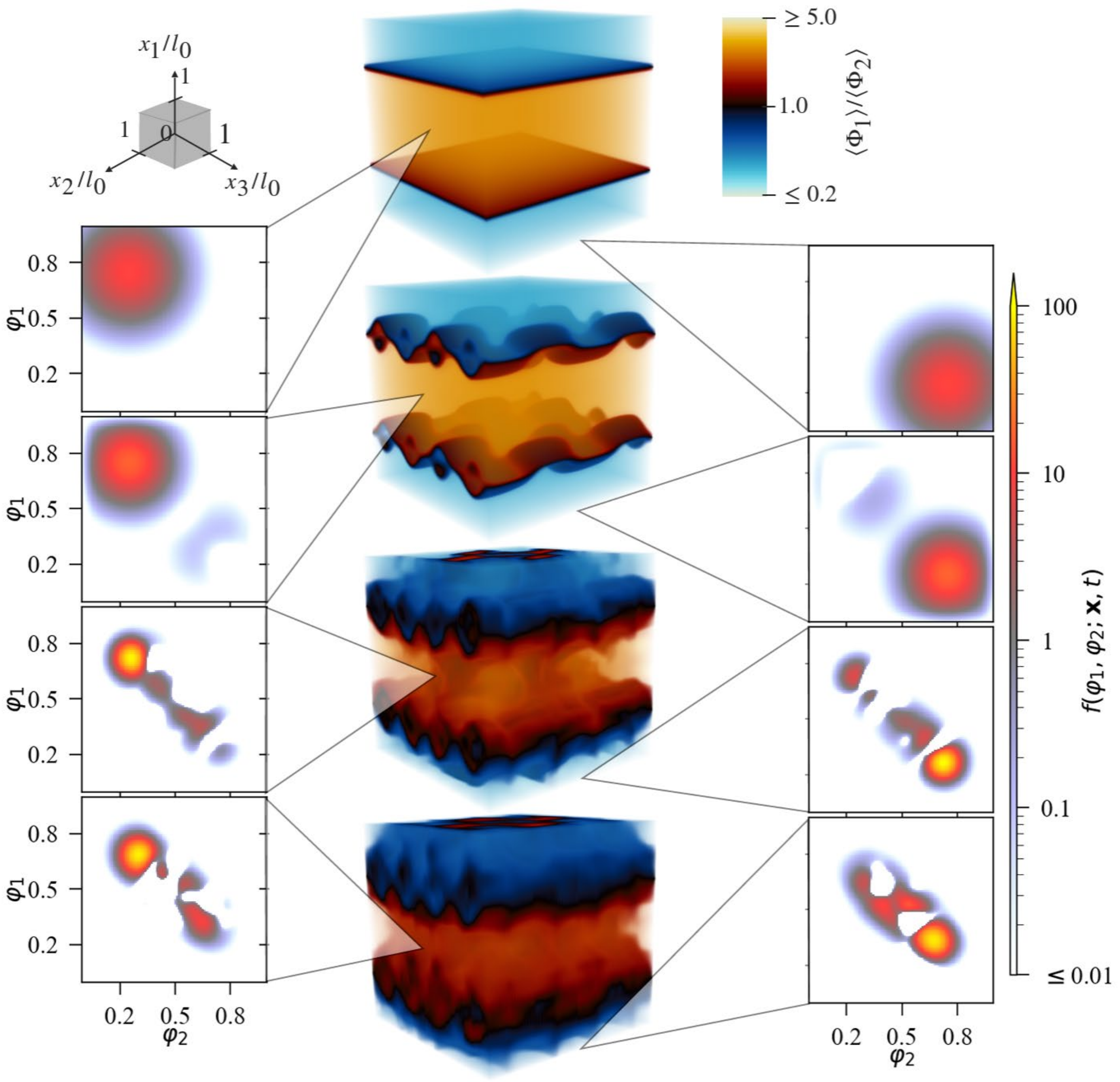

- LES-FDF simulation

  $A + B \rightarrow P$ in 3D

- Grid size: 128^5
- Shown is the dynamical evolution of the joint PDF of two reactants as a function of time

- *Tensor networks enable the calculation of turbulence probability distributions*, Nikita Gourianov, Peyman Givi, Dieter Jaksch, and Stephen B. Pope, Sci. Adv. **11**, eads5990 (2025)

LES Simulation – stochastic closure

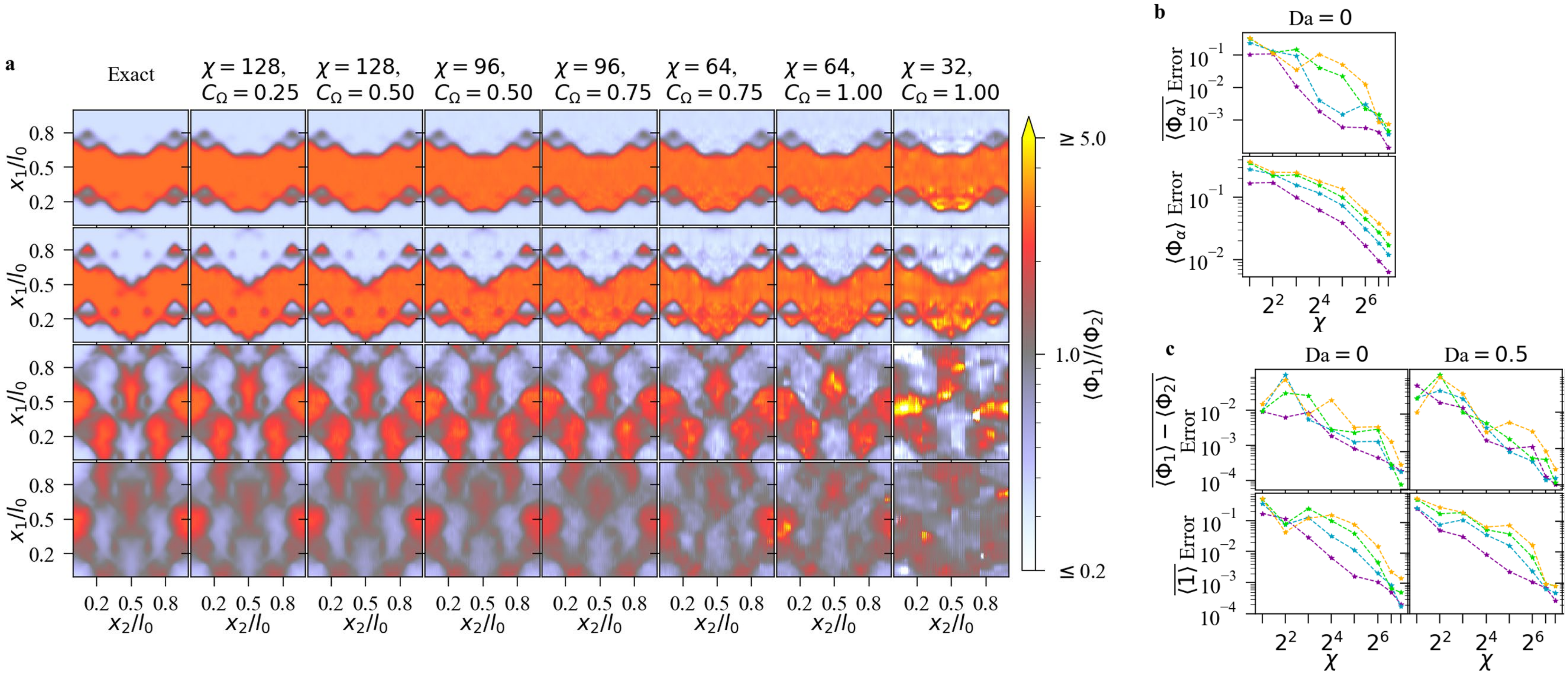

Tensor networks enable the calculation of turbulence probability distributions, N. Gourianov, P. Givi, D. Jaksch, and S.B. Pope, Sci. Adv. **11**, eads5990 (2025)

Final probability distributions on the centre

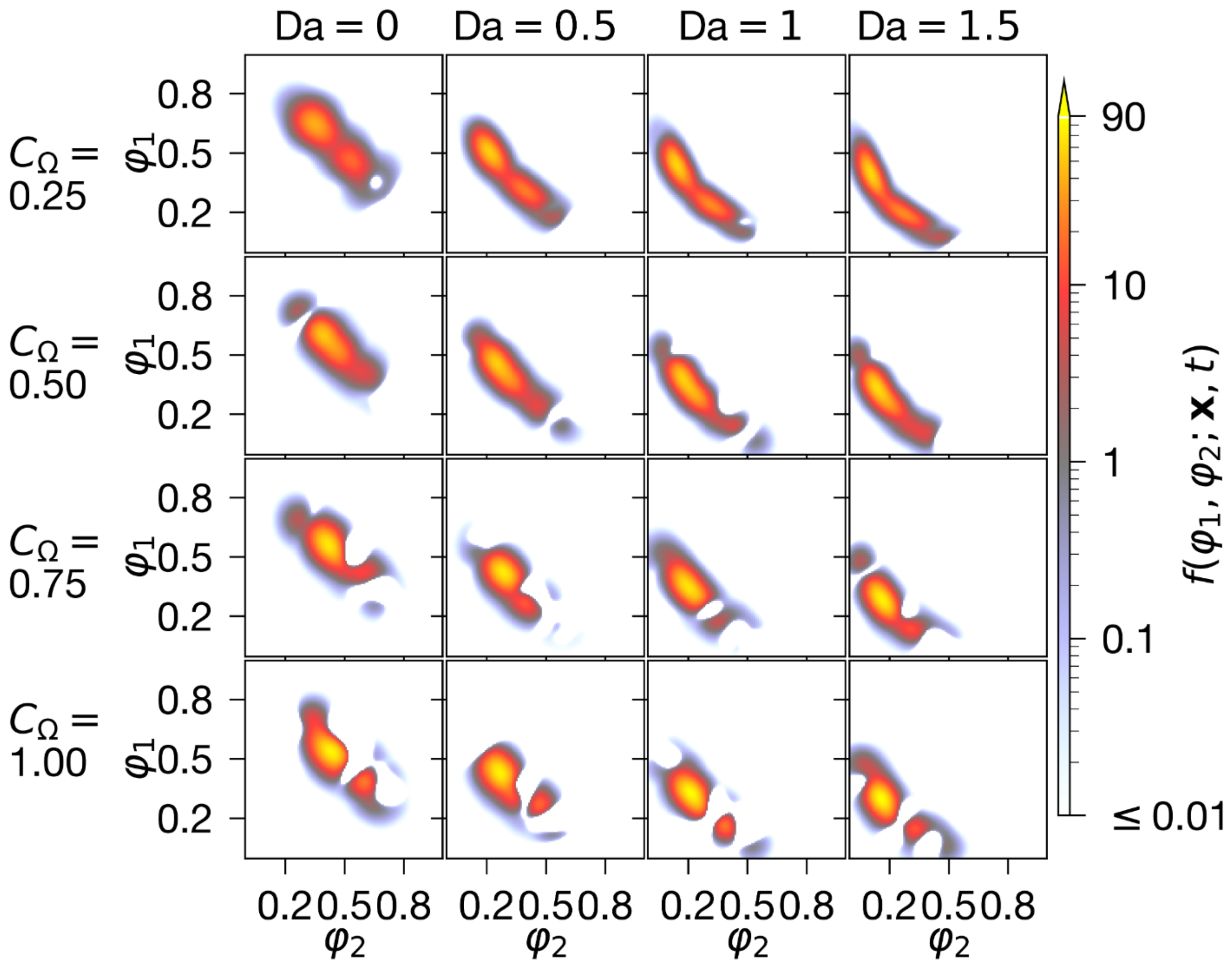

The PDFs at the end of the simulation($t/T0 = 2$) are shown here in the centre of the spatial domain

$x/l0 = (12{,}12{,}12)$

for all combinations of C_Ω, Da. The PDFs are computed using $\chi = 128$ MPS simulations.

Example: Rayleigh-Benard

The Oberbeck-Boussinesq equations

- The equations governing the convection

  $$\partial_t u_i + u_j \partial_j u_i = -\partial_i p + \nu \partial_j^2 u_i + \beta g\, \delta_{i3} \theta,$$

  $$\partial_t \theta + u_j \partial_j \theta = \kappa \partial_j^2 \theta,$$

- ν is the viscosity, β is the thermal expansion coefficient, g the gravitational constant, and κ the thermal diffusivity; all of them are independent of position $\boldsymbol{x}$, time t and temperature.
- $\boldsymbol{u}(\boldsymbol{x}, t)$ is the velocity field, $\theta(\boldsymbol{x}, t)$ the temperature relative to some reference temperature and $p(\boldsymbol{x}, t)$ the kinematic pressure.
- The equations are augmented by

  $$\partial_j u_j = 0$$

- We use a Chorin projection for consistently updating pressure and velocity fields

- The boundary conditions are given by
  - $\boldsymbol{u} = 0$ at all walls
  - $\theta\left(z = \pm\frac{L}{2}\right) = \mp\frac{\Delta}{2}$ at the top and bottom walls
  - $\partial_x \theta = \partial_y \theta = 0$ at the side walls (no heat flow through the side walls)
- The aspect ratio of the box width W to height L is denoted by $\Gamma = \mathrm{W/L}$.
- The dimensionless control parameters are
  - Rayleigh number $\mathrm{Ra} = \frac{\beta g L^3 \Delta}{\kappa \nu}$
  - Prantl number $\mathrm{Pr} = \frac{\nu}{\kappa}$
- Choosing a suitable typical speed U we also define the Reynolds number

  $$\mathrm{Re} = \frac{U}{\nu L^{-1}}$$

System response

- The most important system response is the Nusselt number

$$\mathrm{Nu} = \frac{H}{\lambda \Delta L^{-1}} = \frac{\langle u_z \theta \rangle_{A,t} - \kappa \partial_z \langle \theta \rangle_{A,t}}{\kappa \Delta L^{-1}}$$

- Here H is the heat flux from top to bottom and $\lambda = c_p \rho \kappa$ is the thermal conductivity.

- $\langle \cdots \rangle_{A,t}$ denotes averaging over (any) horizontal plane and time.

- The main question is how far we get with the MPS code and what bond dimension χ is needed.

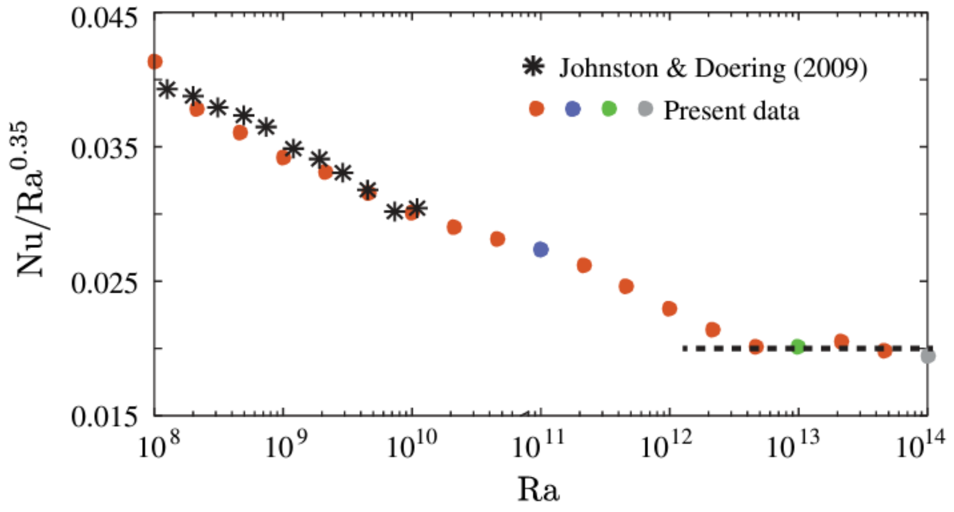

FIG. 1. Nu(Ra) plot compensated by $\mathrm{Ra}^{0.35}$. The data agree well with the previous results in the low-Ra regime [39]. The flow structures of the three colored data points (blue for $\mathrm{Ra} = 10^{11}$, green for $\mathrm{Ra} = 10^{13}$, and gray for $\mathrm{Ra} = 10^{14}$) are displayed in Fig. 2.

These results were obtained in 2D with $\Gamma = 2$ and $\mathrm{Pr} = 1$ using a second-order finite-difference code

MPS solutions Oberbeck-Boussinesq equations

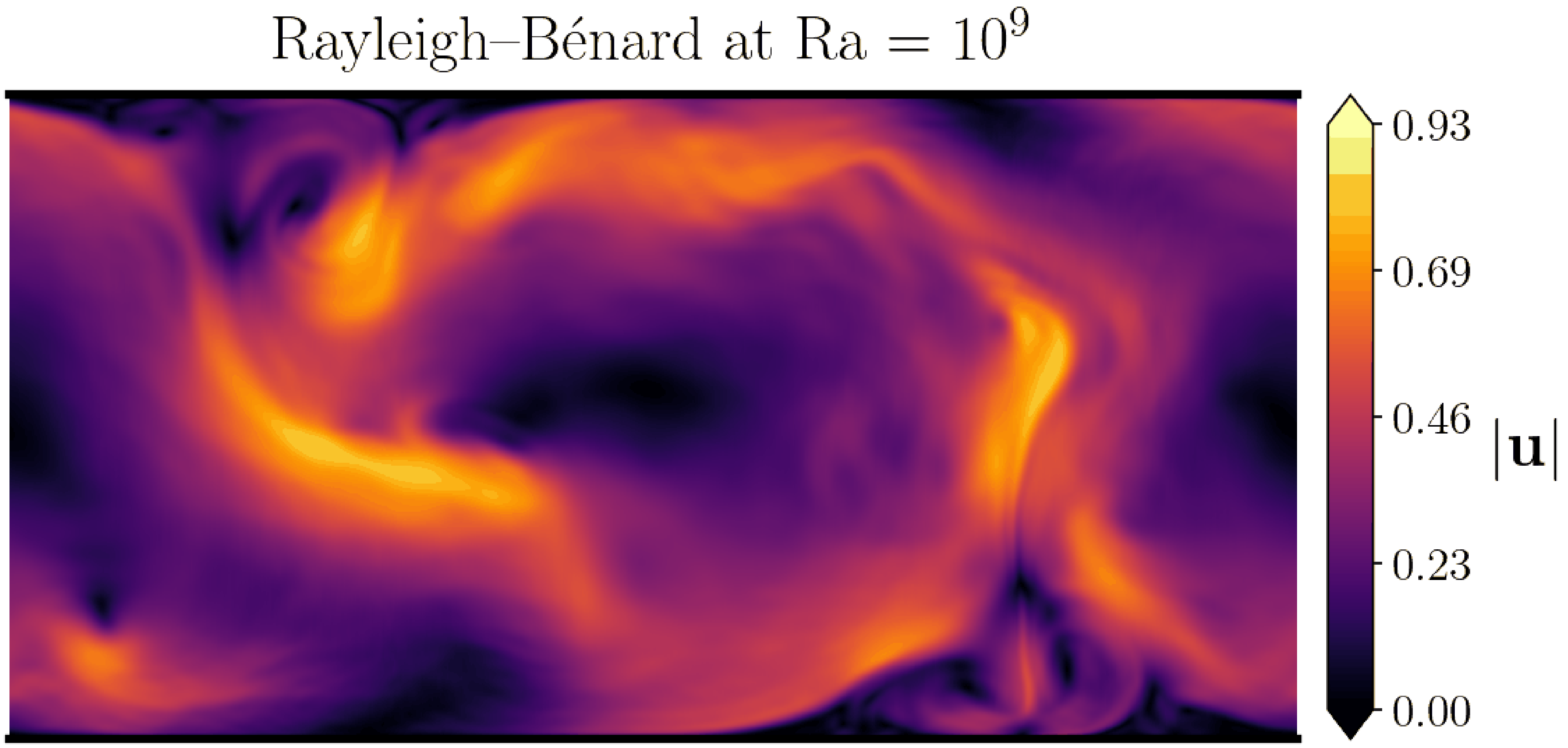

Nusselt number for $Ra = 10^8$

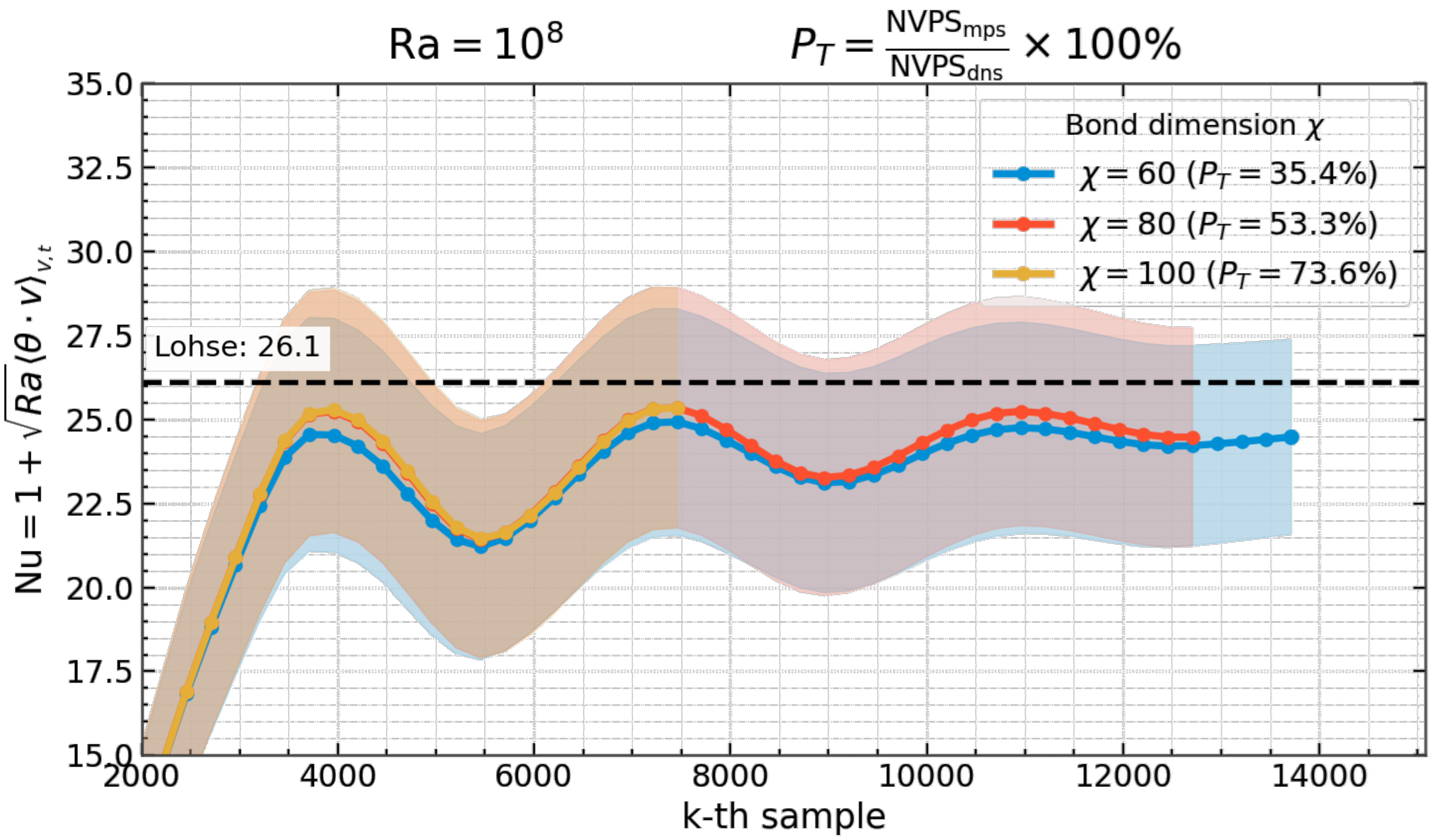

Nis-Luca van Huelst et al., in preparation)

QCFD consortium and collaborations beyond

Dieter Jaksch@UHH
Thomas Rung@TUHH
Felix Motzoi@Juelich
Barbara Kraus@TUM
Dimitris Angelakis@TUC
Paolo Geremia@ENGYS
Martin Kiffner@PlanQC

Steven@Cornell

Nik@OXF

Peyman@PIT

Michael@$\mathcal{Q}$

QCFD

The QCFD project is funded under the EU’s Horizon Programme (HORIZON-CL4-2021-DIGITAL-EMERGING-02-10), Grant Agreement 101080085.

QCFD (qcfd-h2020.eu)

AFOSR
AIR FORCE OFFICE OF SCIENTIFIC RESEARCH

CUI THE HAMBURG CENTRE FOR ULTRAFAST IMAGING
Advanced Imaging of Matter

Related publications

- **MPS encoding and Multigrid Renormalization**
  - M. Lubasch, P. Moinier and D. Jaksch, *Multigrid Renormalization,* J. Comp. Phys. **372**, 587 (2018)
- **Quantum Algorithms for nonlinear optimization**
  - M. Lubasch, J. Joo, P. Moinier, M. Kiffner and D. Jaksch, *Variational Quantum Algorithms for Nonlinear Problems,* Phys. Rev. A **101**, 010301(R) (2020)
- **QCFD and tensor network algorithms**
  - N. Gourianov, M. Lubasch, S. Dolgov, Q.Y. van den Berg, H. Babaee, P. Givi, M. Kiffner and D. Jaksch, *A quantum-inspired approach to exploit turbulence structures,* Nature Computational Science **2**, 30 (2022).
  - D. Jaksch, P. Givi, A.J. Daley and T. Rung, *Variational Quantum Algorithms for Computational Fluid Dynamics*, AIAA Journal **61**, 1885 (2023)
  - M. Kiffner and D. Jaksch, *Tensor network reduced order models for wall-bounded flows*, Phys. Rev. Fluids **8**, 124101 (2023)
  - P. Over, S. Bengoechea, T. Rung, F. Clerici, L. Scandurra, E. de Villiers, D. Jaksch, *Boundary treatment for variational quantum simulations of partial differential equations on quantum computers,* Computers & Fluids **288**, 106508 (2025)
  - N. Gourianov, P. Givi, D. Jaksch, and S.B. Pope, *Tensor networks enable the calculation of turbulence probability distributions*, Sci. Adv. **11**, eads5990 (2025)
  - S. Bengoechea, P. Over, D. Jaksch, and T. Rung, *Towards Variational Quantum Algorithms for generalized linear and nonlinear transport phenomena*, arXiv:2411.14931 (2024)
  - P. Siegl, G.S. Reese, T. Hashizume, N.-L. van Hülst, and D. Jaksch, *Tensor-Programmable Quantum Circuits for Solving Differential Equations*, arXiv:2502.04425 (2025)
  - Nis-Luca van Hülst, Pia Siegl, Paul Over, Sergio Bengoechea, Tomohiro Hashizume, Mario Guillaume Cecile, Thomas Rung, Dieter Jaksch, *Quantum-Inspired Tensor-Network Fractional-Step Method for Incompressible Flow in Curvilinear Coordinates,* arXiv:2507.05222 (2025)

QS